

Anomalies in BatCoV/RaTG13 sequencing and provenance

Daoyu Zhang

ABSTRACT

To this date, the most critical piece of evidence on the purported “natural origin” theory of SARS-CoV-2, was the sequence known as RaTG13, allegedly collected from a single fecal sample from *Rhinolophus Affinis*. Understanding the provenance of RaTG13 is critical on the ongoing debate of the Origins of SARS-CoV-2. However, this sample is allegedly “used up” and therefore can no longer be accessed nor sequenced independently [1], and the only available data was the 3 related Genbank accessions: MN996532.1, SRX7724752 and SRX8357956.

We report these datasets possessed multiple significant anomalies, and the provenance of the promised claims of RaTG13 or its role in proving a “probable bat origin”[2] of SARS-CoV-2 can not be satisfied nor possibly be confirmed.

RESULTS

Anomalous enrichment of telomere-like repeat sequences in the dataset SRX7724752

```
>gn|SRA|SRR11085797.3.1 3 (Biological)
```

```
CTAACCCCTAACCCCTAGCACTATCCTGTTTCCAACCCCAACCCCTAACCCCTCACCCCTAACCC  
TAACCCCGAGCCTGTTTCATACCTTAACCTCGCACCTCATCGCTAACCCCGAGCCCTCACCCG  
ATCCTGTTTCTCTCCCGAACATAACCCCT
```

```
>gn|SRA|SRR11085797.3.2 3 (Biological)
```

```
GGTTAGGGTTAGGGTTAGGGTTGGAACAGGATAGGGTTAGGGTTAGGGTTAGGGTTAGGGTTAGG  
GTTAGAGTTAGGGTTGGAAACAGGATAGGGTTAGGGTTAGGGCGAGGGATAGGGATAGGG  
AGGGAAACAGGATAGTGGGAGGGCTAGGGGT
```

>gnl|SRA|SRR11085797.8.1 8 (Biological)

GTTAGGGTTAGGGTTAGGGTTAGGGTTGGGTTGGATACAGGATATGGTTAGGGTTAGGG
GTAGGGTCAGGGTTAGGATTGGAAACGAGATAGGTTACGTGATAGGGTTAGCGTTAGGGT
TAGGTTTAGTAATCCGCAACGGCTTAGGGTT

>gnl|SRA|SRR11085797.8.2 8 (Biological)

CCTAACCCTAACCCTAACCCTAACCCTAACCCTAACCCTAACCCATCCTGTTCCCAACCCTAACC
CTAACCCTAACCCTAACCCTAACACAAAACATAACCCTAACCCCAACCCAAACCCTAACC
CCATCTTTACTCACACCCTAACCCAAAACCTC

>gnl|SRA|SRR11085797.10.1 10 (Biological)

GTTAGGGTTAGGGTTAGCGTTAGGGTTAGAAACAGGATAGGGTTAGGGTTAGGGTTAGGG
TTAGGGTTTTGGTTGGTCACAGTGTTCGCTAGGCATAGGGATAGGGTTCCGTTAGGGT
TAGGGTTAGGATTCGGAAGAGCTAGCTAAA

>gnl|SRA|SRR11085797.10.2 10 (Biological)

GTTCCCAACCCTAACCCTAACCCTAACCCTAACCCTAACCCTTTCCTTTTTCCAACCCTA
ACACTAACCCTAACACTAACCCTAACCCCAACCCTACCCTATACTATATCCGACTCTCA
CGCTAACACTAACATAAGTAATCACAATT

>gnl|SRA|SRR11085797.13.1 13 (Biological)

TAACCCTAACCCTAAGCGTAAACCTAATCCAATCCTGTTCCCAACCCTAACCCTAACCCCT
GACCCTAAGCTTTTTCCCGACCCGAACGCCGACCCGATCCGCCACCCTAACCGTAACCCGT
TCCCAACCCCTCCTACTGCTCGATCCGCCT

>gnl|SRA|SRR11085797.13.2 13 (Biological)

GGAACAGGATAGGGTTAGGGTTAGGGTTAGGGTTAGGGTTAGGGTTAGGGTTAGGGTTAGGG
GTTAGGGTTAGGGTTGGGATCAGGATAGGGATAGGGATAGGGATAGGGATAGGGTTAGGG
TGGGGAACAGGAGAGCGTTAGGCAAGG

>gnl|SRA|SRR11085797.14.1 14 (Biological)

GGTTAGGGTTAGGGTTGGAGAAGAGGATAGGTTTAGGGTTTAGGGTTAGGGTTAGGGTTAGGG
GTTAGGGGAGAGGGTTAGCTACACGATAGGAGTAGGGTAACGATTAGGGTTAGGGTTAGGT
TTGGAAAAAGCATAGGCTATGAGGTACGGT

>gnl|SRA|SRR11085797.14.2 14 (Biological)

CTGCTTCCAACCCTAACCCTAACCCTAACCCTAACCCTAACCCTAACCCTAACCCTAACCCTAACC
CTATCCTGTTCCCAACCCTAACCCTAACCCTAACCCCAACCCTAACCCCAACCCAAACCCCT
AACCCTAACCCCAACCCATACCCCAACCAT


```

>gnl|SRA|SRR11085797.20.1 20 (Biological)
CCTGTTTCCAACCCCTCACCCTGACACTGACCCTAACACTAACCCTAACCCGATC
CTGTTTCTGACCCTAACGACAAGCCTGGCACTAAACTGATCGCGTTTCCAATCGTTACCG
CTTCCCTAACACCCGTCTGTGAAGATACTCCG

>gnl|SRA|SRR11085797.20.2 20 (Biological)
CTTTAGGTTTAGTGTAGGGATAGGGTTAGGGTTAGGGTTAGGGTTAGGGTTAGGGTTAG
GGTTGGGAACAGGATAGGGTTAGGGTTAGGGATAGGGTTGGGGTCTGGATAGGGTTGGGG
GTAGGGTTAGAGTGAGTGTGGGCAGCAGCG

```

Figure 1: The reads that contained Telomere-like repeat sequences within the first 20 reads of SRX7724752.

Despite the theoretical presence of traces of Telomere-like repeats in total RNA of most cells, such repeats comprise only a tiny fraction of the total cellular RNA within real biological samples, and normally does not show up in the first 100 reads. RaTG13 contained an anomalous amount of such repeats, which comprises 63% of the dataset and exist in nearly any set of 10 reads within this dataset. In comparison, the next highest content of such repeats within any other sample of similar context on NCBI, contained merely 4% of these repeats, which does not show up in the first 20 reads of the dataset. Telomere-like repeats are not detected in the first 100 reads of any other datasets examined.

In comparison, the related SRX7724693 lacked such reads within the first 100 reads of the dataset.

```

>gnl|SRA|SRR11085736.100.1 100 (Biological)
CTACTGTGTCATCCCATTTCCAAACGCATTATTGGCGGTACAGGAATATCAACCTGTTGT
CCATCACCTACGCCTTTCGGCCTCGGCTTAGGTCTCTGACTAACCCAGGGCAGAAGAACCT
TCCCCCTGGAAACCTTGGGTGACGGCCCCGTG

>gnl|SRA|SRR11085736.100.2 100 (Biological)
ATCCACGGGCCGTAAACCCAAAGGTTTCCAGGGGAAGGTTTCGTCCGCCCTGGGTAGTCA
GGACCTAAGCCGACGCCGAAAGGCGTAGGTGATGGACAACAGGTTGATATTCCTGTAACC
GCAATAAGCGTTTGAGAGATGGGATGACAGT

```

Figure 2: the first 100 reads in SRX7724693 did not show any Telomere-like repeats.

In addition, SRX7724752 contained 6% all-N sequences that were exactly 35nt long, which is not found at levels any close in other datasets that had the same design section.

Reads (separated)

```

>gnl|SRA|SRR11085797.11.1 11 (Biological)
NNNNNNNNNNNNNNNNNNNNNNNNNNNNNNNNNNNNNNNNNNNNNNNNNNNNNNNNNNNN
>gnl|SRA|SRR11085797.11.2 11 (Biological)
NNNNNNNNNNNNNNNNNNNNNNNNNNNNNNNNNNNNNNNNNNNNNNNNNNNNNNNNNNNN

```

Figure 3: an example of All-N read in SRX7724752.

Anomalous enrichment of non-attributable and low-match data within SRX7724752

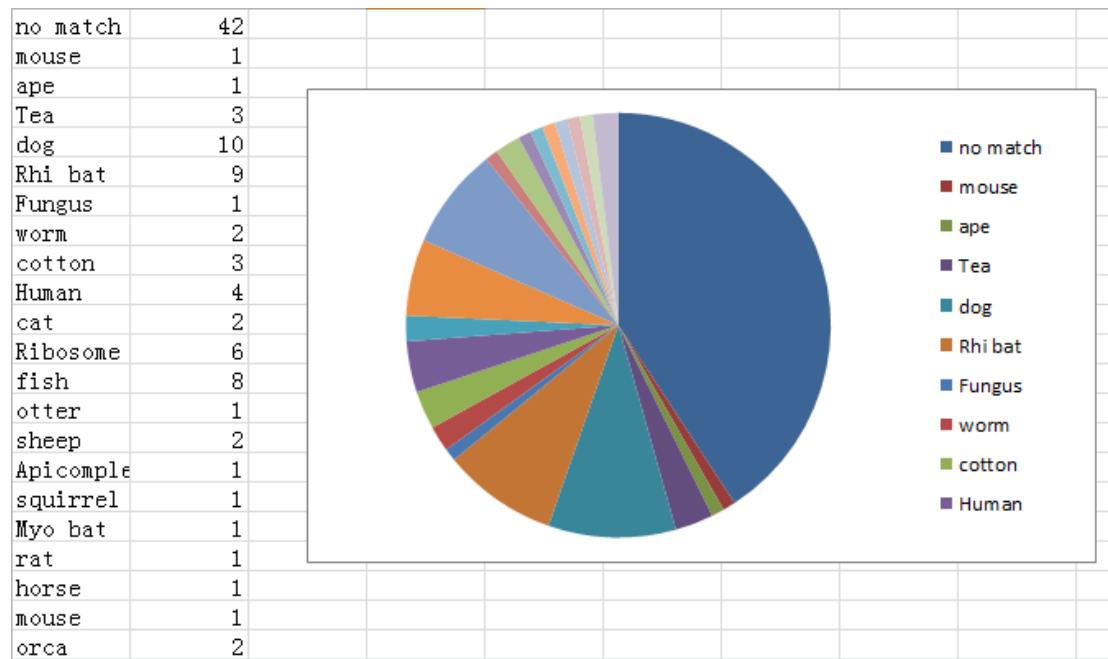


Figure 4: BLAST result of 100 random reads obtained from RaTG13 using BLASTn.

In addition to the anomalous enrichment of repeats, The vast majority of the non-repeat sequences in SRX7724752 does not show any clear matches when examined using BLASTn. With matching results ranging from nearly all domains of life—all of which were partial and low-quality matches, including that of bats.

Only 2 out of 7 Non-repeat and non-PolyN sequences from the first 20 reads from SRX7724752 had any matches, and the match was only partial matches to certain hypothetical proteins

Description

Molecule type

Query Length

Other reports [Distance tree of results](#) [MSA viewer](#) [?](#)

Percent Identity to

E value to

Query Coverage to

[Filter](#) [Reset](#)

Descriptions | [Graphic Summary](#) | [Alignments](#) | [Taxonomy](#)

Sequences producing significant alignments Download Manage Columns Show [?](#)

select all 6 sequences selected [GenBank](#) [Graphics](#) [Distance tree of results](#)

Description	Max Score	Total Score	Query Cover	E value	Per. Ident	Accession
<input checked="" type="checkbox"/> Eimeria mitis hypothetical protein conserved partial mRNA	102	102	44%	4e-18	94.03%	XM_013494305.1

Results for: 1:lc|Query_61914 gn|SRA|SRR11085797.7.1.7 (Biological)(150bp) ▼

Program: BLASTN [Citation](#) ▼

Database: nt [See details](#) ▼

Query ID: lc|Query_61914

Description: gn|SRA|SRR11085797.7.1.7 (Biological)

Molecule type: dna

Query Length: 150

Other reports: [Distance tree of results](#) ?

Organism: *only top 20 will appear* exclude

Type common name, binomial, taxid or group name

[+ Add organism](#)

Percent Identity: to

E value: to

Query Coverage: to

[Filter](#) [Reset](#)

Descriptions | [Graphic Summary](#) | [Alignments](#) | [Taxonomy](#)

Sequences producing significant alignments | [Download](#) ▼ | [Manage Columns](#) ▼ | Show: 5000 ▼ ?

select all 2 sequences selected

[GenBank](#) | [Graphics](#) | [Distance tree of results](#)

Description	Max Score	Total Score	Query Cover	E value	Per. Ident	Accession
<input checked="" type="checkbox"/> Eimeria mitis hypothetical protein_conserved partial mRNA	73.1	73.1	40%	3e-09	88.33%	XM_013494305.1
<input checked="" type="checkbox"/> Cyprinus carpio genome assembly common caro genome_scaffold 000012284	73.1	73.1	40%	3e-09	88.33%	LN595243.1

Figure 5: the BLASTn result of the 2 non-repeat and non-PolyN sequences in the first 20 reads of SRX7724752. The rest can not be matched to any known organisms.

Depletion of bacterial-like reads in SRX7724272 which is inconsistent with fecal samples prepared using the methods as indicated by the “Design” section of the SRX7724752 metadata.

Fecal matter [3], is primarily bacteria by composition. All other fecal swabs prepared using the methods indicated by the metadata correctly showed the presence of bacteria as the majority of the reads. In contrast, SRX7724272 contained only 0.65% bacteria-like reads, all of which were 16S rRNA.

discernible reads from bacterial mRNA.

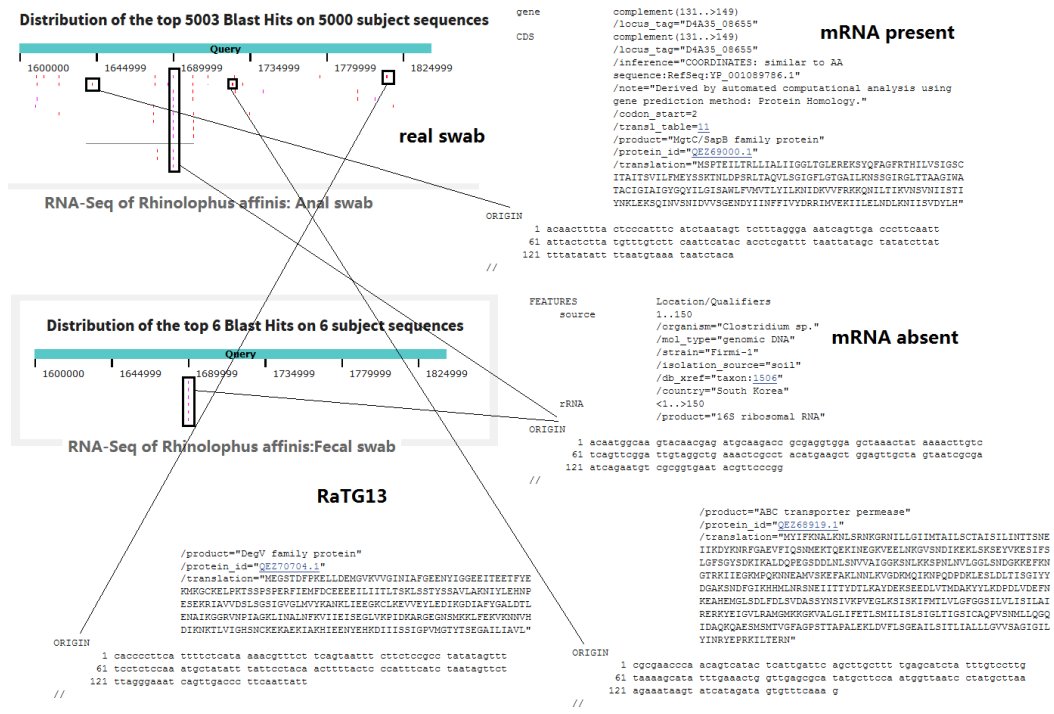


Figure 8: BLAST hits of bacterial non-ribosomal RNA genome on SRX7724272 and another swab from Rhinolophus Affinis under the same library preparation section.

Observation of anomalous and unexpected data within SRX7724752

```

>gnl|SRA|SRR11085797.11550005.1 11550005 (Biological)
GCCCGTATTTAGCCTTAGATGGAGTTTACCACCCGCTTTGGGCATTCACCAAGCAACC
CGACTCCGGGAAGACCCGGGCCCGCGCCGGGGCCGCTACCGGCCTCACACCGTCCA
CGGGCTGGGCCTCGATCAGAAGGACTTGGGC

>gnl|SRA|SRR11085797.11550005.2 11550005 (Biological)
CGGTGGGGCGCGGGACATTTGGCGTACGGAAGACCCACTCCCCGGCGCCGCTCGTGGGGG
CCCAAGTCCCTTCGATCGAGGCCAGCCCGTGGACGGTGTGAGGCCGGTAGCGGCCCCCG
CGCGCCGGGCCCGGGTCTTCCCGGAGTCCG

```

Description

gn|SRA|SRR11085797.11550005.1 11550005 (B ...

Molecule type

dna

Query Length

151

Other reports

[Distance tree of results](#) [MSA viewer](#) [?](#)

Descriptions | Graphic Summary | Alignments | Taxonomy

Sequences producing significant alignments Download Manage Columns Show 100 ?

select all 100 sequences selected [GenBank](#) [Graphics](#) [Distance tree of results](#)

	Description	Max Score	Total Score	Query Cover	E value	Per. Ident	Accession
<input checked="" type="checkbox"/>	PREDICTED: Phyllostomus discolor 28S ribosomal RNA (LOC114512504)_rRNA	279	279	100%	2e-71	100.00%	XR_003685809.1
<input checked="" type="checkbox"/>	PREDICTED: Phyllostomus discolor basic proline-rich protein-like (LOC114512442)_mRNA	279	279	100%	2e-71	100.00%	XM_028531404.1
<input checked="" type="checkbox"/>	Homo sapiens lncAB370.3 lncRNA gene complete sequence	274	274	100%	9e-70	99.34%	MK280359.1
<input checked="" type="checkbox"/>	Homo sapiens lncAB366.1 lncRNA gene complete sequence	274	274	100%	9e-70	99.34%	MK280356.1
<input checked="" type="checkbox"/>	Felis catus Senzu DNA_chromosome: E1_American Shorthair breed	274	1372	100%	9e-70	99.34%	AP023165.1
<input checked="" type="checkbox"/>	PREDICTED: Marmota flaviventris 28S ribosomal RNA (LOC117794687)_rRNA	274	274	100%	9e-70	99.34%	XR_004618536.1
<input checked="" type="checkbox"/>	PREDICTED: Avicanthus niloticus 28S ribosomal RNA (LOC117704856)_rRNA	274	274	100%	9e-70	99.34%	XR_004606369.1
<input checked="" type="checkbox"/>	PREDICTED: Avicanthus niloticus 28S ribosomal RNA (LOC117704855)_rRNA	274	274	100%	9e-70	99.34%	XR_004606368.1

Description gn|SRA|SRR11085797.11550005.1 11550005 (Biological)
Molecule type dna
Query Length 151
Other reports [Distance tree of results](#) [MSA viewer](#) [?](#)

Percent Identity to **E value** to **Query Coverage** to

Descriptions | Graphic Summary | Alignments

Sequences producing significant alignments Download Manage Columns Show 100 ?

select all 100 sequences selected [Graphics](#) [Distance tree of results](#)

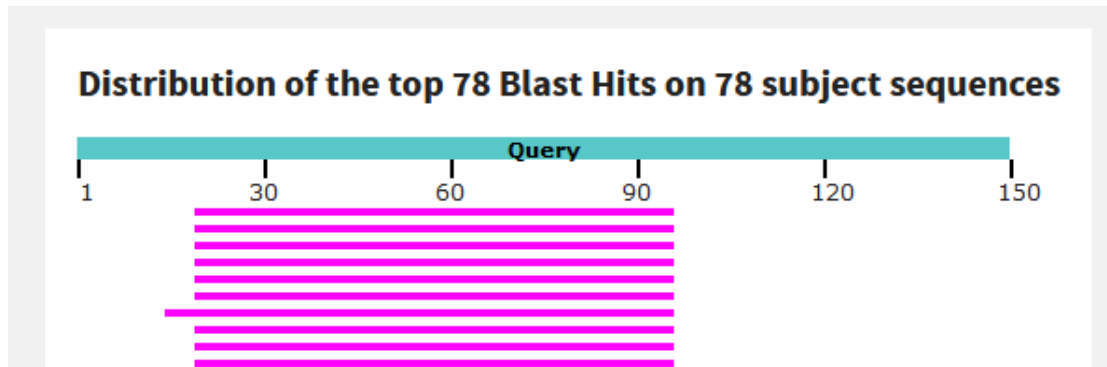
	Description	Max Score	Total Score	Query Cover	E value	Per. Ident	Accession
<input checked="" type="checkbox"/>	SRX7724752	279	279	100%	2e-73	100.00%	SRA:SRR11085797.11601488.1
<input checked="" type="checkbox"/>	SRX7724752	279	279	100%	2e-73	100.00%	SRA:SRR11085797.11595932.1
<input checked="" type="checkbox"/>	SRX7724752	279	279	100%	2e-73	100.00%	SRA:SRR11085797.11598985.1
<input checked="" type="checkbox"/>	SRX7724752	279	279	100%	2e-73	100.00%	SRA:SRR11085797.11598757.1
<input checked="" type="checkbox"/>	SRX7724752	279	279	100%	2e-73	100.00%	SRA:SRR11085797.11588533.1
<input checked="" type="checkbox"/>	SRX7724752	279	279	100%	2e-73	100.00%	SRA:SRR11085797.11585765.1
<input checked="" type="checkbox"/>	SRX7724752	279	279	100%	2e-73	100.00%	SRA:SRR11085797.11585419.1
<input checked="" type="checkbox"/>	SRX7724752	279	279	100%	2e-73	100.00%	SRA:SRR11085797.11583582.1
<input checked="" type="checkbox"/>	SRX7724752	279	279	100%	2e-73	100.00%	SRA:SRR11085797.11582051.1
<input checked="" type="checkbox"/>	SRX7724752	279	279	100%	2e-73	100.00%	SRA:SRR11085797.11580259.1
<input checked="" type="checkbox"/>	SRX7724752	279	279	100%	2e-73	100.00%	SRA:SRR11085797.11579956.1
<input checked="" type="checkbox"/>	SRX7724752	279	279	100%	2e-73	100.00%	SRA:SRR11085797.11579609.1
<input checked="" type="checkbox"/>	SRX7724752	279	279	100%	2e-73	100.00%	SRA:SRR11085797.11573984.1
<input checked="" type="checkbox"/>	SRX7724752	279	279	100%	2e-73	100.00%	SRA:SRR11085797.11570618.1
<input checked="" type="checkbox"/>	SRX7724752	279	279	100%	2e-73	100.00%	SRA:SRR11085797.11568464.1
<input checked="" type="checkbox"/>	SRX7724752	279	279	100%	2e-73	100.00%	SRA:SRR11085797.11567362.1
<input checked="" type="checkbox"/>	SRX7724752	279	279	100%	2e-73	100.00%	SRA:SRR11085797.11566985.1
<input checked="" type="checkbox"/>	SRX7724752	279	279	100%	2e-73	100.00%	SRA:SRR11085797.11558788.1



Pale spear-nosed bat

Figure 9: *Phyllostomus Discolor*, or Pale spear-nosed bat, a species of bat native to the Americas, is found in high abundance within SRX7724752.

```
>gnl|SRA|SRR11085797.11550023.2 11550023 (Biological)
TTTGTTTTGTTTTTATAATTTATTTTTAAAATTTATTGGGGTGACAATTGTTAGTAAAA
TTACATAGATTTTCAGGTGTACAATTCCTGTATTACATGTGGACGGTCCAGCCGCCACGAGT
TCAACGTTTTACATGAAAGGGGGTGTGGGA
```



[Download](#) [GenBank](#) [Graphics](#)

Rhinolophus ferrumequinum clone VMRC7-331J24, complete sequence

Sequence ID: [AC150242.3](#) Length: 120894 Number of Matches: 1

Range 1: 32707 to 32786 [GenBank](#) [Graphics](#)

[Next Match](#) [Previous Match](#)

Score	Expect	Identities	Gaps	Strand	
122 bits(66)	3e-24	76/80(95%)	3/80(3%)	Plus/Plus	
Query 20	tttattttttaa---at	tttattGGGGTGACA	ATTGTTAGTAAAA	TACATAGATTTCAGG	76
Sbjct 32707	TTTTTTTTTAAATTT	ATTTATTTGGGGTG	ACAATTGTTAGTAA	AATTACATAGATTT	CAGG 32766
Query 77	TGTACAATTCCTGT	ATTACAT			96
Sbjct 32767	TGTACAATTCCTGT	ATTACAT			32786

Figure 10: A sequence which was matched to a bat mRNA clone in the first 96 nucleotides, but then matching nothing on the later nucleotides. This match end with a T.

Bat coronavirus RaTG13, complete genome

Sequence ID: [MN996532.1](#) Length: 29855 Number of Matches: 2

Range 1: 26736 to 26844 [GenBank](#) [Graphics](#) [Next Match](#) [Previous Match](#)

Score	Expect	Identities	Gaps	Strand
161 bits(87)	7e-36	102/109(94%)	2/109(1%)	Plus/Plus
Query 45	GCAC	TGACTTG-CTT-TAGCACTGATGTGGCTGAGCTACTTCATTGCTTCTTTCAGGCTA		102
Sbjct 26736	GCAATGGCTTGTCTTGTAGGCTTGATGTGGCTGAGCTACTTCATTGCTTCTTTCAGGCTA			26795
Query 103	TTTGCACGTACGCGTTCCATGTGGTCATTCAATCCAGAACTAACATTT			151
Sbjct 26796	TTTGCACGTACGCGTTCCATGTGGTCATTCAATCCAGAACTAACATTT			26844

Range 2: 27478 to 27542 [GenBank](#) [Graphics](#) [Next Match](#) [Previous Match](#) [First Match](#)

Score	Expect	Identities	Gaps	Strand
121 bits(65)	1e-23	65/65(100%)	0/65(0%)	Plus/Plus
Query 1	ATGAAGGCAATTCACCATTCCATCCTCTAGCTGATAATAAATTTGCACTGACTTGCTTTA			60
Sbjct 27478	ATGAAGGCAATTCACCATTCCATCCTCTAGCTGATAATAAATTTGCACTGACTTGCTTTA			27537
Query 61	GCACT 65			
Sbjct 27538	GCACT 27542			

Figure 12: an anomalous fusion of two non-canonical regions of the RaTG13 genome. The fusion again happens on a T.

Bat coronavirus RaTG13, complete genome

Sequence ID: [MN996532.1](#) Length: 29855 Number of Matches: 2

Range 1: 28217 to 28346 [GenBank](#) [Graphics](#) [Next Match](#) [Previous Match](#)

Score	Expect	Identities	Gaps	Strand
233 bits(126)	2e-57	129/130(99%)	1/130(0%)	Plus/Plus
Query 23	TTC-TCTAAACGAACAACTAAAATGTCTGATAATGGACCCCAAAACCAACGAAATGCAC			81
Sbjct 28217	TTCATCTAAACGAACAACTAAAATGTCTGATAATGGACCCCAAAACCAACGAAATGCAC			28276
Query 82	CCCGCATTACGTTTGGTGGACCCTCAGATTCAACTGGCAGTAACCAGAATGGAGAACGCA			141
Sbjct 28277	CCCGCATTACGTTTGGTGGACCCTCAGATTCAACTGGCAGTAACCAGAATGGAGAACGCA			28336
Query 142	GTGGAGCACG 151			
Sbjct 28337	GTGGAGCACG 28346			

Range 2: 25 to 60 [GenBank](#) [Graphics](#) [Next Match](#) [Previous Match](#) [First Match](#)

Score	Expect	Identities	Gaps	Strand
67.6 bits(36)	2e-07	36/36(100%)	0/36(0%)	Plus/Plus
Query 1	CTCTCGATCTCTTGTAGATCTGTCTCTAAACGAAC		36	
Sbjct 25	CTCTCGATCTCTTGTAGATCTGTCTCTAAACGAAC		60	

Figure 13: the only canonical sgRNA-like read* in SRX7724752. Furthermore, SRX7724752 contained significant amount of reads that had higher query coverage on the DNA sequence than on the corresponding mRNA. This most likely indicate a clonal, rather than cDNA, library, was responsible for most of the bat-like reads observed in SRX7724752.

```

>gnl|SRA|SRR11085797.76.1 76 (Biological)
CATCAAAC TGAGGTTTCAGCAAGGCAAAGATAGCCAGCAACAAAACAAAAGGCATCCTA
CTGAATGGAAGCAGATAATTGCCAATAGTACATCAGTAAGGAGTTAATATTAAGAATTAG
TTTTTAAAAAGCTCTATATGATGTCAGAAAT

>gnl|SRA|SRR11085797.76.2 76 (Biological)
GTTTTTCAC TTGCATTTCTCTAATAAATTAGTGATGTTGAGCATCTTTTCATATGTCATTTG
GCCATCTGTATGTCGTCTTTGGAGAAATGTCATATTCAGATTTCTGCCCAATTTTAATTG
GCTTGTTTTGTTTTTTGTTTTTTGAATTGAGTT

```

Descriptions Graphic Summary Alignments Taxonomy

Sequences producing significant alignments Download Manage Columns Show 100

select all 11 sequences selected GenBank Graphics Distance tree of results

	Description	Max Score	Total Score	Query Cover	E value	Per. Ident	Accession
<input checked="" type="checkbox"/>	Rhinolophus ferrumequinum clone VMRC7-71A7 . complete sequence	267	267	99%	1e-67	98.68%	AC150307.3
<input checked="" type="checkbox"/>	Rhinolophus ferrumequinum clone VMRC7-251C10 . complete sequence	185	185	94%	4e-43	90.14%	AC149630.3
<input checked="" type="checkbox"/>	Myotis lucifugus clone CH235-427D16 . complete sequence	137	137	82%	1e-28	87.20%	AC174832.3
<input checked="" type="checkbox"/>	Pteropus alecto clone BAC.P100M20 .BAC.P103A18 . complete sequence	135	135	86%	4e-28	85.38%	KP862827.1
<input checked="" type="checkbox"/>	Pteropus alecto clone BAC.P201M3 .BAC.P216K21 . complete sequence	135	135	86%	4e-28	85.38%	KP862826.1
<input checked="" type="checkbox"/>	Pteropus alecto clone BAC.P56N20 . complete sequence	135	135	86%	4e-28	85.38%	KP862825.1
<input checked="" type="checkbox"/>	Rhinolophus euryale isolate REM0134 microsatellite RM1198 . sequence	128	128	47%	7e-26	98.61%	KC910215.1
<input checked="" type="checkbox"/>	Pteropus alecto clone BAC.P212O7-1 .BAC.P229M21 . complete sequence	126	126	84%	3e-25	84.38%	KP862828.1
<input checked="" type="checkbox"/>	PREDICTED: Miniopterus natalensis zinc finger protein 713 (ZNF713) . transcript variant X3 . mRNA	106	106	90%	3e-19	81.02%	XM_016196283.1
<input checked="" type="checkbox"/>	PREDICTED: Miniopterus natalensis zinc finger protein 713 (ZNF713) . transcript variant X2 . mRNA	106	106	90%	3e-19	81.02%	XM_016196281.1
<input checked="" type="checkbox"/>	PREDICTED: Miniopterus natalensis zinc finger protein 713 (ZNF713) . transcript variant X1 . mRNA	106	106	90%	3e-19	81.02%	XM_016196280.1

Figure 14: a read from SRX7724752 which have higher coverage on the clone than on the corresponding mRNA. E.g. the read contained nucleotide sequences that were not supposed to be transcribed in actual cells/bats.

Inability of SRX8357956 to prove the promises claimed in [5]

Date	RaTG13		SARS-CoV-2		Sequence	Blast Archive	Name
	Identity	Query Cover	Identity	Query Cover			
14-Oct-18	95.53%	56%	93.15%	56%	24	archive.is/H107n	gnl SRA SRR11806578.24 RaTG13-9-5-5_9-5-f1_2018-10-14_B02
14-Oct-18	97.31%	76%	93.18%	75%	23	archive.is/8phs4	gnl SRA SRR11806578.23 RaTG13-9-5-4_9-5-r1_2018-10-14_C02
14-Oct-18	97.55%	53%	93.00%	52%	25	archive.is/ycQ89	gnl SRA SRR11806578.25 RaTG13-9-5-5_9-5-r1_2018-10-14_D02
14-Oct-18	99.43%	97%	96.39%	97%	22	archive.is/abSp6	gnl SRA SRR11806578.22 RaTG13-9-5-4_9-5-f1_2018-10-14_A02
11-Oct-18	97.37%	98%	92.23%	98%	20	archive.is/B20Et	gnl SRA SRR11806578.20 RaTG13-9-5-1_21230-F_2018-10-11_A12
11-Oct-18	98.54%	99%	88.26%	99%	21	archive.is/L2pTq	gnl SRA SRR11806578.21 RaTG13-9-5-1_23258-R_2018-10-11_B12
08-Oct-18	98.64%	98%	96.19%	99%	5	archive.is/W7Fxp	gnl SRA SRR11806578.5 RaTG13-11-2_18297-F_TSS20181008-027-0303_G10
08-Oct-18	99.19%	98%	91.83%	98%	7	archive.is/h8810	gnl SRA SRR11806578.7 RaTG13-12-2_24144-R_TSS20181008-027-0303_C11
08-Oct-18	99.89%	99%	87.86%	99%	6	archive.is/VJY2	gnl SRA SRR11806578.6 RaTG13-12-2_22717-F_TSS20181008-027-0303_H10
30-Sep-18	99.50%	99%	92.71%	99%	9	archive.is/ONBUX	gnl SRA SRR11806578.9 RaTG13-2-3_RaTG13-2-R1_2018-09-30_B11
30-Sep-18	99.79%	99%	92.89%	99%	8	archive.is/udSil	gnl SRA SRR11806578.8 RaTG13-2-3_RaTG13-2-F_2018-09-30_A02
29-Sep-18	99.00%	99%	94.20%	99%	10	archive.is/jdzvN	gnl SRA SRR11806578.10 RaTG13-2-3_RaTG13-2-R2_2018-09-29_D05
29-Sep-18	99.09%	98%	94.97%	98%	3	archive.is/lI99e	gnl SRA SRR11806578.3 RaTG13-10-3_RaTG13-10-F_2018-09-29_G04
29-Sep-18	99.72%	98%	98.06%	98%	11	archive.is/7Kioa	gnl SRA SRR11806578.11 RaTG13-20-1_RaTG13-F_2018-09-29_H04
29-Sep-18	99.72%	98%	95.19%	98%	4	archive.is/tKXGj	gnl SRA SRR11806578.4 RaTG13-10-3_RaTG13-10-R_2018-09-29_E05
27-Sep-18	95.03%	98%	90.88%	98%	14	archive.is/NNfnm	gnl SRA SRR11806578.14 RaTG13-4-2_RaTG13-4-R_2018-09-27_G06
27-Sep-18	95.82%	98%	93.46%	93%	13	archive.is/udSil	gnl SRA SRR11806578.13 RaTG13-4-2_RaTG13-4-F_2018-09-27_G05
27-Sep-18	98.08%	98%	94.50%	98%	1	archive.is/kcHAi	gnl SRA SRR11806578.1 RaTG13-1-2_RaTG13-1-F_2018-09-27_E05
27-Sep-18	98.81%	99%	96.90%	99%	17	archive.is/nhvd2	gnl SRA SRR11806578.17 RaTG13-6-2_RaTG13-6-R_2018-09-27_H06
27-Sep-18	98.91%	99%	94.54%	99%	2	archive.is/veLPW	gnl SRA SRR11806578.2 RaTG13-1-2_RaTG13-1-R_2018-09-27_F06
27-Sep-18	99.09%	99%	96.92%	99%	16	archive.is/dtqMp	gnl SRA SRR11806578.16 RaTG13-6-2_RaTG13-6-F_2018-09-27_A06
27-Sep-18	99.28%	98%	96.81%	98%	12	archive.is/ZHjMY	gnl SRA SRR11806578.12 RaTG13-3-2_RaTG13-3-F_2018-09-27_F05
27-Sep-18	99.46%	98%	96.74%	98%	15	archive.is/Epig7	gnl SRA SRR11806578.15 RaTG13-5-2_RaTG13-5-F_2018-09-27_H05
27-Sep-18	99.50%	98%	98.49%	98%	18	archive.is/NdyHK	gnl SRA SRR11806578.18 RaTG13-7-2_RaTG13-7-F_2018-09-27_B06
27-Sep-18	99.53%	99%	95.67%	97%	19	archive.is/2qg0a	gnl SRA SRR11806578.19 RaTG13-8-2_RaTG13-8-F_2018-09-27_C06
20-Jun-17	99.10%	99%	96.61%	99%	28	archive.is/ve7nN	gnl SRA SRR11806578.28 RaTG13-R-1-1_7896-1-F1_2017-06-20_E03
20-Jun-17	99.61%	99%	97.43%	99%	32	archive.is/ehzBr	gnl SRA SRR11806578.32 RaTG13-R-4-1_7896-4-F_2017-06-20_F03
20-Jun-17	99.87%	98%	97.42%	98%	33	archive.is/do9Rt	gnl SRA SRR11806578.33 RaTG13-R-4-1_7896-4-R_2017-06-20_H03
20-Jun-17	99.90%	98%	97.44%	98%	29	archive.is/HjQD8	gnl SRA SRR11806578.29 RaTG13-R-1-1_7896-1-R1_2017-06-20_G03
17-Jun-17	98.56%	99%	95.85%	99%	26	archive.is/fqWWF	gnl SRA SRR11806578.26 RaTG13-ORF8-1-1_ORF8-F_2017-06-17_A05
17-Jun-17	98.99%	98%	96.52%	98%	27	archive.is/N01Ah	gnl SRA SRR11806578.27 RaTG13-ORF8-1-1_ORF8-R1_2017-06-17_A06
03-Jun-17	99.07%	97%	97.49%	97%	30	archive.is/WwyWy	gnl SRA SRR11806578.30 RaTG13-R-2-1_7896-2-F1_2017-06-03_A07
03-Jun-17	99.46%	99%	98.01%	99%	31	archive.is/tCLHu	gnl SRA SRR11806578.31 RaTG13-R-2-1_7896-2-R1_2017-06-03_A08

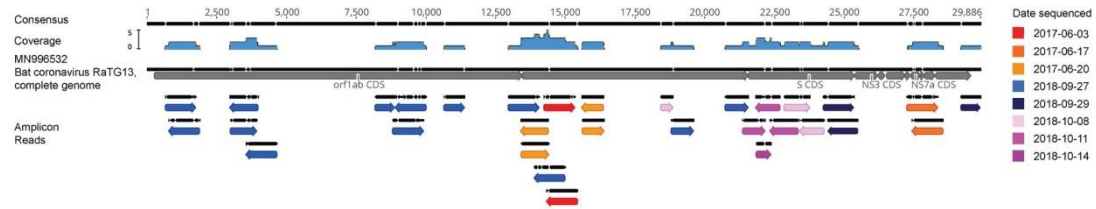


Figure 15: A complete analysis [4] of all Amplicon sequences in SRX8357956. Including the location of these amplicons and the similarity of such amplicon to the RaTG13 and SARS-CoV-2 genome.

Chuan Xiao et.al claimed that RaTG13 contained all the 3 S1 variable loops that were previously considered unique in SARS-CoV-2. [5] However, such claims can not be verified using the amplicons listed in SRX8357956.

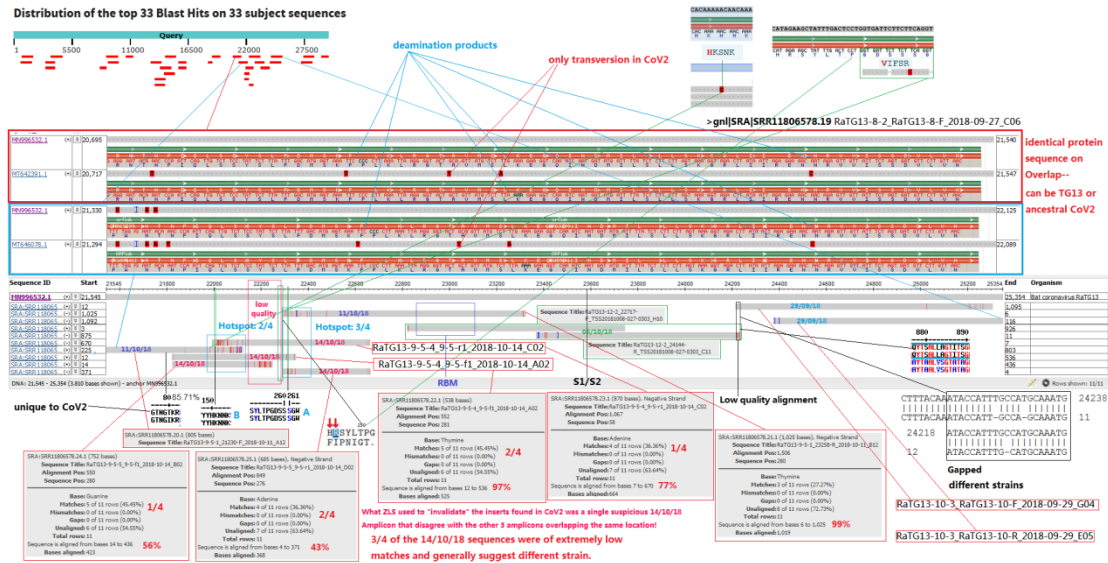


Figure 16: a thorough analysis of the amplicons located on the S locus of RaTG13 in SRX8357956. Notice that the last 4 amplicons sequenced in 14/10/2018 was of very low quality matches, and matched other organisms—including Mouse(mus musculus).

select all 99 sequences selected

Description	Max Score	Total Score	Query Cover	E value	Per. Ident	Accession
<input checked="" type="checkbox"/> Gadus morhua genome assembly_chromosome: 16	60.8	105	27%	4e-05	78.05%	LR633958.1
<input checked="" type="checkbox"/> Mus musculus BAC clone RP24-498P8 from chromosome 9_complete sequence	59.9	59.9	47%	1e-04	72.92%	AC168217.2
<input checked="" type="checkbox"/> Mus musculus chromosome 9_clone RP24-484G16_complete sequence	59.9	59.9	47%	1e-04	72.92%	AC137678.11

select all 100 sequences selected

Description	Max Score	Total Score	Query Cover	E value	Per. Ident	Accession
<input checked="" type="checkbox"/> Homo sapiens BAC clone RP11-792A8 from 7_complete sequence	54.5	54.5	44%	0.006	71.15%	AC027644.9
<input checked="" type="checkbox"/> Coregonus sp. 'balchen' genome assembly_chromosome: 7	52.7	52.7	29%	0.022	73.68%	LR778259.1
<input checked="" type="checkbox"/> Coregonus sp. 'balchen' genome assembly_chromosome: 15	50.9	50.9	16%	0.078	83.33%	LR778267.1
<input checked="" type="checkbox"/> Salmo trutta genome assembly_chromosome: 21	50.9	50.9	37%	0.078	71.90%	LR584437.1
<input checked="" type="checkbox"/> Xanthophyllomyces dendrorhous genome assembly_Xden1_scaffold Scaffold_79	50.9	50.9	9%	0.078	96.88%	LN483167.1
<input checked="" type="checkbox"/> Coregonus sp. 'balchen' genome assembly_chromosome: 20	50.0	50.0	72%	0.078	67.49%	LR778272.1
<input checked="" type="checkbox"/> Aquila chrysaetos chrysaetos genome assembly_chromosome: 14	50.0	141	42%	0.078	69.50%	LR606194.1
<input checked="" type="checkbox"/> Bos mutus isolate yakQH1 chromosome 16	50.0	50.0	24%	0.078	74.68%	CP027084.1
<input checked="" type="checkbox"/> Mus musculus BAC clone RP23-128D11 from 7_complete sequence	50.0	50.0	36%	0.078	71.90%	AC122222.6
<input checked="" type="checkbox"/> Mus musculus BAC clone RP23-66E21 from 7_complete sequence	50.0	50.0	36%	0.078	71.90%	AC131741.4

select all 24 sequences selected

Description	Max Score	Total Score	Query Cover	E value	Per. Ident	Accession
<input checked="" type="checkbox"/> Mus musculus targeted KO-first_conditional ready_lacZ-tagged mutant allele Fabp4.tm1a(KOMP)Wts	50.9	50.9	23%	0.045	85.11%	JN963014.1
<input checked="" type="checkbox"/> Mus musculus targeted non-conditional_lacZ-tagged mutant allele Fabp4.tm1e(KOMP)Wtsj_transger	50.9	50.9	23%	0.045	85.11%	JN947213.1
<input checked="" type="checkbox"/> Mus musculus chromosome 3_clone RP23-436F15_complete sequence	50.9	50.9	23%	0.045	85.11%	AC123726.11
<input checked="" type="checkbox"/> Mus musculus chromosome 3_clone RP24-137C19_complete sequence	50.9	50.9	23%	0.045	85.11%	AC113990.10

Figure 16: BLAST result of the non-RaTG13 matched parts of Amplicons 25, 24 and 23 in SRX8357956. Using the remaining amplicons, the 3 variable loops, GTNGIKR, HKSNNK and VIFSQ was obtained.

This is vastly different from the variable loops possessed by SARS-CoV-2, which were GTNGTKR, HKNNK and GDSSSG. Therefore, the promise of Chuan Xiao et. Al does not hold upon raw data analysis.

Probable discontinuities in RaTG13 sequencing in SRX8357956

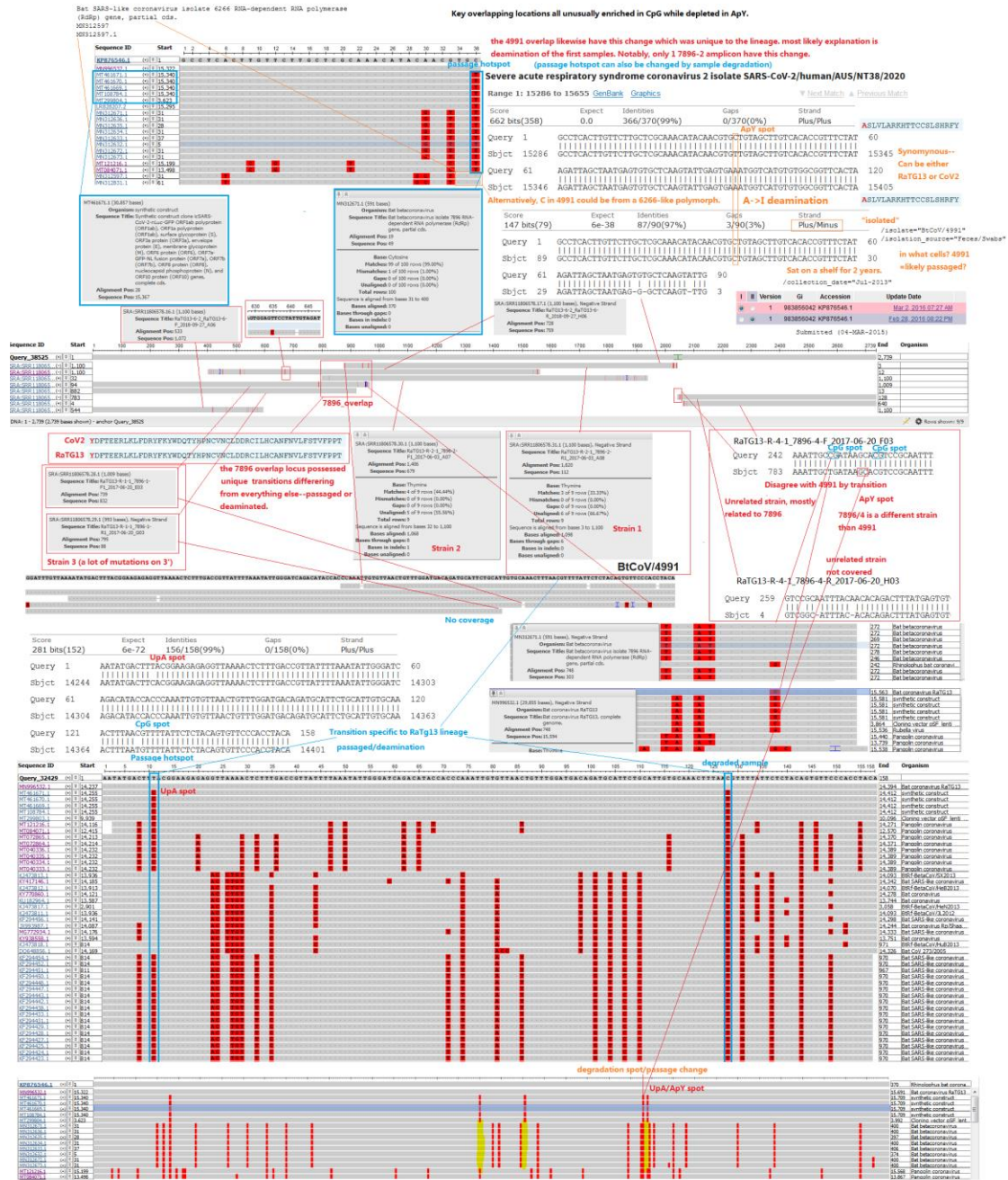


Figure 17: Detailed analysis of the early amplicons located in the nsp12 RdRp region of RaTG13 in SRX8357956.

Within the amplicons labeled “7896”, there were 2 sites of overlap—the first overlap, a region 158bp in length, contained only 2nt difference—all C-T transitions—to SARS-CoV-2. Such transitions easily arise in passage, and are probable sequencing errors from a degraded/passaged sample of DNA.

The second overlap, one with BtCoV/4991, contained only 1 C-T transition, which have a probable origin in the primers used to generate the amplicons in the first place.

DISCUSSIONS

Origins of the anomalies in SRX7724752

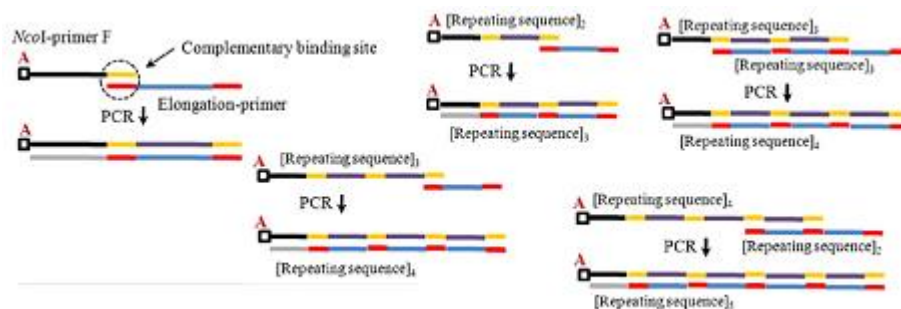


Figure 18A: Origin of repeating sequences in SRX7724752.

The only satiable explanation for the anomalous enrichment of the Telomere-like repeats in SRX7724752, involves the self-amplification of such sequences in a PCR reaction with little to no template.

Normally, with significant amount of template, the random primers normally used in RT-PCR amplifies most sequences evenly and outcompetes the repeat sequences in the reaction, and the result was an accurate reflection of such repeats within cellular samples—extremely poor. However, in samples that have little to no template, such that the random primers/random hexamers used in the reaction were not able to prime the amplification of most sequences—e.g. the amount of normal templates within the reaction falls below the timescale needed for the amplification of the repeating sequences, Repeating sequences, of which telomere-like repeats forms the vast majority of it in the environment and in most samples, can self-amplify in a primer-independent fashion, eventually reaching very high dominance, through repeated denaturing, sliding, reannealing and extension.

As this is a linear process, the self-amplification process is very slow, and is normally outcompeted by the normal amplicons as long as any usable amount of templates were present. Therefore, the presence of anomalously enriched telomere-like repeats within SRX7724752 indicate that the original sample couldn't have contained enough templates for the generation of the complete genome, through any means possible.

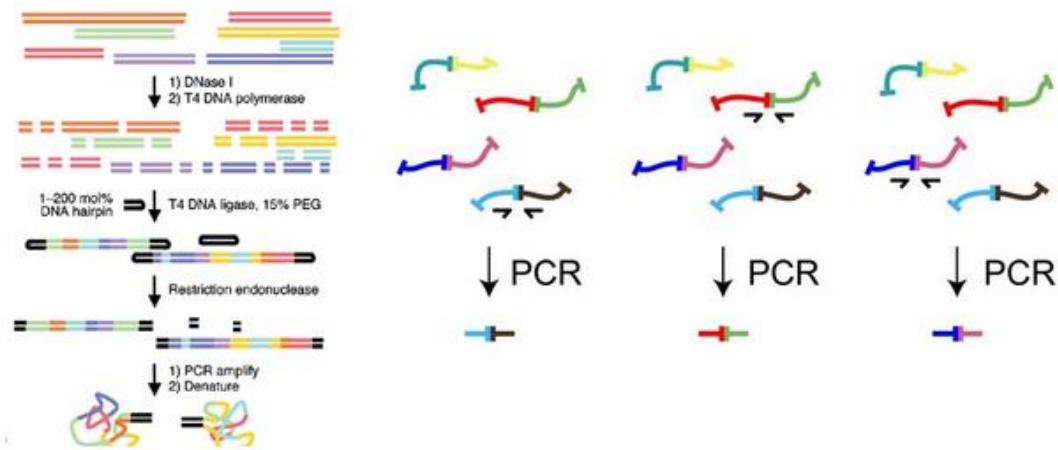


Figure 18B: Origin of the random matched sequences and partial sequences in SRX7724752
 The majority of the sequences that were not repeats, when BLASTed, does not match any known organisms. There were also many sequences that matches—only partially, to many diverse organisms. What was striking, is, however, is that these matches often ends with an “A” or a “T”. The most possible explanation of this anomaly is that the Library preparation process of ILLUMINA RNA-seq, which include strand synthesis and A-T ligation to adaptors, were fed dsDNA rather than ssRNA, as input. Such dsDNA input may be PCR products, or it may be a pre-made ILLUMINA sequencing library—Certain mRNA-like reads were inadvertently inverted, indicating double-stranded cDNA was likely used instead of single stranded mRNA.

RID	J85DMESK016 Search expires on 08-01 20:59 pm Download All ▼
Results for	2:lcl Query_5937 gnl SRA SRR11085797.66.2 66 (Biological)(150bp) ▼
Program	BLASTN ? Citation ▼
Database	nt See details ▼
Query ID	lcl Query_5937
Description	gnl SRA SRR11085797.66.2 66 (Biological)
Molecule type	dna
Query Length	150
Other reports	Distance tree of results ?

Download ▾ GenBank Graphics

PREDICTED: Hipposideros armiger putative P2Y purinoceptor 10 (LOC109385656), mRNA

Sequence ID: [XM_019648164.1](#) Length: 2682 Number of Matches: 1

Range 1: 2162 to 2293 [GenBank](#) [Graphics](#) [Next Match](#) [Previous Match](#)

Score	Expect	Identities	Gaps	Strand
154 bits(83)	1e-33	116/132(88%)	1/132(0%)	Plus/Minus
Query 12	TTT-TCATTATTAAGTATTATGTACTGTACATAAATGTATGTACTATACTTTTATACAAC	70		
Sbjct 2293	TTTATCATATCAAGTGTATGTACTGTACAGTATGTATGTGTATATACTTTTATATGAC	2234		
Query 71	TGGCAGCACAGCAGGTTTGGTTTATACCAGCATCACCACAAAAATGTGAGTAAATGCATTAC	130		
Sbjct 2233	TGACAGCATAGTAGGCTTGGTTTACACCAGCATCACCACAAAAATGTGAGTAAATGCATTAC	2174		
Query 131	ACTACAATGTTA	142		
Sbjct 2173	ACTATGATGTTA	2162		

Figure 19: An inverted mRNA-like read.

*: Analysis of the sole sgRNA-like read reveal the usage of a leader/F primer and the mispriming of Amplicon DNA

```

          ttagatttcattctaaacgaacaaactaaaatgtctgataatggacccccaaacgaatgcacccccgattacgtttgggtgacccct
          CTCTCGATCTCTGTAGATCTGTTCTCTAAACGAAC
ACA AACCAACGAACCTCTCGATCTCTGTAGATCTGTTCTCTAAACGAAC
          TAACTCCTTTTIGCCCTAGTTTACCGATCTCATCGCCCTGCCAGGGTCCATGGACTGTGTGATCTGCTCTCTGCTCCTC

```

Figure 20a: the match analysis between different genomic fragments of RaTG13, of the sole sgRNA-like read* in SRX7724752. *:Figure 13

Despite being sgRNA-like in the first glance, analysis of the exact overlapping region of this particular read reveal that this region is identical to BtCoV/ZC45 and BtCoV/ZXC21—indicating it's identity as likely being a consensus primer.

select all 100 sequences selected

	Description	Max Score	Total Score	Query Cover	E value	Per. Ident	Accession
<input checked="" type="checkbox"/>	Pangolin coronavirus isolate PCoV_GX-P3B_genomic_sequence	67.6	67.6	100%	8e-09	100.00%	MT072865.1
<input checked="" type="checkbox"/>	Pangolin coronavirus isolate PCoV_GX-P2V_complete_genome	67.6	67.6	100%	8e-09	100.00%	MT072864.1
<input checked="" type="checkbox"/>	Pangolin coronavirus isolate PCoV_GX-P5E_complete_genome	67.6	67.6	100%	8e-09	100.00%	MT040336.1
<input checked="" type="checkbox"/>	Pangolin coronavirus isolate PCoV_GX-P5L_complete_genome	67.6	67.6	100%	8e-09	100.00%	MT040335.1
<input checked="" type="checkbox"/>	Pangolin coronavirus isolate PCoV_GX-P1E_complete_genome	67.6	67.6	100%	8e-09	100.00%	MT040334.1
<input checked="" type="checkbox"/>	Pangolin coronavirus isolate PCoV_GX-P4L_complete_genome	67.6	67.6	100%	8e-09	100.00%	MT040333.1
<input checked="" type="checkbox"/>	Bat coronavirus RaTG13_complete_genome	67.6	67.6	100%	8e-09	100.00%	MN996532.1
<input checked="" type="checkbox"/>	Bat SARS-like coronavirus isolate bat-SL-CoVZXC21_complete_genome	67.6	67.6	100%	8e-09	100.00%	MG772934.1
<input checked="" type="checkbox"/>	Bat SARS-like coronavirus isolate bat-SL-CoVZC45_complete_genome	67.6	67.6	100%	8e-09	100.00%	MG772933.1
<input checked="" type="checkbox"/>	Bat coronavirus (BtCoV/279/2005)_complete_genome	65.8	65.8	97%	3e-08	100.00%	DQ648857.1
<input checked="" type="checkbox"/>	Mutant SARS coronavirus Urbani clone SARS-Urbani-MA_SHC014-spike_complete_genome	63.9	63.9	94%	1e-07	100.00%	MT308984.1
<input checked="" type="checkbox"/>	Coronavirus BtRs-BetaCoV/YN2018D_complete_genome	63.9	63.9	94%	1e-07	100.00%	MK211378.1

Figure 20b: BLAST result of CTCTCGATCTCTGTAGATCTGTTCTCTAAACGAAC.

This particular sequence have extended overlap to the beginning of the N gene, which was coincidentally at the end of the last 2017/06/17 amplicon. This indicate it was most likely the product of mispriming, rather than a true sgRNA-like read.

SRX7724752 is a mixed library consists of a matrix of dried American bat guano, a bat WGS/RNA-seq ILLUMINA library, a synthetic 16S library and megaprimer PCR products from the SRX8357956 Amplicons and a degraded sample of SARS-CoV-2 cDNA

Phyllostomus Discolor, a species of bat native to Mexico and southern United states, leaves numerous Full-length 100% matched reads that don't match anything else. Coincidentally, Mexico is one of the major supplier of bat guano used for fertilizer and other commercial purposes[6]. The confirmed presence of this particular bat species, suggest the use of a commercial dried bat guano matrix as the bulk of the sample being sequenced. As in PRJNA494391[7] which synthetic metagenome samples were constructed using cDNA amplicons and a specific material matrix to simulate realistic metagenomic reads of a desired virus in a sample.

Traces of the original template used in the megaprimer PCR process can be seen as traces of low-matched virus-like reads within this dataset, which are found across the entire RaTG13 genome.



Figure 21: Read coverage of SRX7724752 on the RaTG13 genome. The red pixels represent significant mismatches on the reads in the dataset.

The Bacterial-like reads in SRX7724752 is also likely a synthetic 16S library—as the only other dataset with Telomere-like repeats(4%), still contained significant amount of bacterial mRNA.

```
>gnl|SRA|SRR11085733.2232944.1 2232944 (Biological)
GCCTTCGTTTGATATAGTTTTAATGCAAATCCCCTAACATCTCTTTCAGCATCTGCTGC
ACCTCTTTCACCAGCAACTGTAGAAAATCTTAAAAGGGCTTTTGTTTTTTTACCAACTTT
GTTAAAAATATCTGCTTTAGAATATTTTGT

>gnl|SRA|SRR11085733.2232944.2 2232944 (Biological)
AGAGGTCCACTCTTTTACAAGATACTTGGCTTTTAGAAAACTTGCACATTTTCGATAGG
GAAAGGATACCAGAAAGAGTTGTGCACGCTAAAGGAAGTGCTGCATACGGCGAATTAACA
ATTACTAATGATATTACAAAATATTCATAA
```


Job Title	AE017125:Helicobacter hepaticus ATCC 51449,...
RID	J88SF43U01R Search expires on 08-01 21:56 pm Download All ▾
Program	? Citation ▾
Database	SRA See details ▾
Query ID	AE017125.1
Description	Helicobacter hepaticus ATCC 51449, complete genome
Molecule type	nucleic acid
Query Length	934935
Other reports	?

 No significant similarity found. For reasons why, [click here](#)

Figure 22b: the same species of bacteria in SRX7724752. No significant matches were found. This dataset is likely subjected to probe-capture sequencing similar to these other datasets—the use of a positive-sense CoV probe resulted in the selective presentation of the negative ssDNA strand of the ligation products to show up. This is supported by the observation that while most of the virus-like reads were on the negative strand, the Repeats does not show a bias in strand polarity, and the mRNA-like reads have a much higher chance of being on the wrong polarity for RNA-seq. This is likely due to the ligation process being used.

Probable signs of laboratory manipulation of SRX7724752

[< Edit Search](#) [Save Search](#) [Search Summary](#) ▾

Job Title [gb|AC097711.2|](#)

RID [KJ2J1YCV01R](#) Search expires on 08-17 18:28 pm [Download All](#) ▾

Program BLASTN [?](#) [Citation](#) ▾

Database SRA [See details](#) ▾

Query ID [AC097711.2](#)

Description Homo sapiens BAC clone RP11-162K6 from 4, complete sequence

Molecule type nucleic acid

Query Length 114657

Other reports [Distance tree of results](#) [MSA viewer](#) [?](#)

[? How to read this report?](#) [▶ BLAST Help Videos](#) [↶ Back to Traditional Results Page](#)

Filter Results

Organism *only top 20 will appear* exclude

Type common name, binomial, taxid or group name

[+ Add organism](#)

Percent Identity to **E value** to **Query Coverage** to

[Filter](#) [Reset](#)

Descriptions [Graphic Summary](#) [Alignments](#)

Sequences producing significant alignments [Download](#) ▾ [Manage Columns](#) ▾ Show [?](#)

select all 100 sequences selected [Graphics](#) [Distance tree of results](#)

Description	Max Score	Total Score	Query Cover	E value	Per. Ident	Accession
<input checked="" type="checkbox"/> SRX7724752	279	279	0%	1e-70	100.00%	SRA_SRR11085797.11044608.2
<input checked="" type="checkbox"/> SRX7724752	279	279	0%	1e-70	100.00%	SRA_SRR11085797.11044608.1

Job Title **gnl|SRA|SRR11085797.11044608.1 11044608**

RID [KJ2FPOKE014](#) Search expires on 08-17 18:27 pm [Download All](#) ▾

Results for ▾

Program **BLASTN** [Citation](#) ▾

Database **nt** [See details](#) ▾

Query ID **lc|Query_54299**

Description **gnl|SRA|SRR11085797.11044608.2 11044608 (Biological)**

Molecule type **dna**

Query Length **151**

Other reports [Distance tree of results](#) ⓘ

Filter Results

Organism *only top 20 will appear* exclude

[+ Add organism](#)

Percent Identity to

E value to

Query Coverage to

[Filter](#) [Reset](#)

Descriptions | [Graphic Summary](#) | [Alignments](#) | [Taxonomy](#)

Sequences producing significant alignments [Download](#) ▾ [Manage Columns](#) ▾ Show ▾ ⓘ

select all 11 sequences selected [GenBank](#) [Graphics](#) [Distance tree of results](#)

Description	Max Score	Total Score	Query Cover	E value	Per. Ident	Accession
<input checked="" type="checkbox"/> Homo sapiens BAC clone RP11-162K6 from 4 complete sequence	279	279	100%	2e-71	100.00%	AC097711.2
<input checked="" type="checkbox"/> Canis lupus familiaris breed Labrador retriever chromosome 32a	274	274	100%	9e-70	99.34%	CP050598.1
<input checked="" type="checkbox"/> Canis lupus familiaris breed Labrador retriever chromosome 32b	274	274	100%	9e-70	99.34%	CP050634.1
<input checked="" type="checkbox"/> Aquila chrysaetos chrysaetos genome assembly_chromosome_1	257	257	100%	9e-65	97.35%	LR606181.1
<input checked="" type="checkbox"/> Apteryx australis mantelli genome assembly_AptMant0_scaffold176	257	257	100%	9e-65	97.35%	LK064748.1
<input checked="" type="checkbox"/> Erithacus rubecula genome assembly_chromosome_5	252	252	100%	4e-63	96.69%	LR812107.1
<input checked="" type="checkbox"/> Anas platyrhynchos genome assembly_chromosome_4	252	252	100%	4e-63	96.69%	LS423614.1
<input checked="" type="checkbox"/> Streptopelia turtur genome assembly_chromosome_4	246	246	100%	2e-61	96.03%	LR594554.1
<input checked="" type="checkbox"/> Mus musculus BAC clone RP24-204J10 from 5 complete sequence	243	243	98%	3e-60	95.97%	AC121929.2
<input checked="" type="checkbox"/> Sciurus carolinensis genome assembly_chromosome_15	204	204	78%	1e-48	97.48%	LR738605.1
<input checked="" type="checkbox"/> PREDICTED: Meleagris gallopavo uncharacterized LOC104910685 (LOC104910685)_mRNA	121	121	45%	1e-23	98.53%	XM_019615117.2

[← Edit Search](#) [Save Search](#) [Search Summary](#) ▾

Job Title **gnl|SRA|SRR11085797.11044608.1 11044608**

RID [KJ2FPOKE014](#) Search expires on 08-17 18:27 pm [Download All](#) ▾

Results for ▾

Program **BLASTN** [Citation](#) ▾

Database **nt** [See details](#) ▾

Query ID **lc|Query_54298**

Description **gnl|SRA|SRR11085797.11044608.1 11044608 (Biological)**

Molecule type **dna**

Query Length **151**

Other reports [Distance tree of results](#) ⓘ

ⓘ How to read this report? [BLAST Help Videos](#) [Back to Traditional Results Page](#)

Filter Results

Organism *only top 20 will appear* exclude

[+ Add organism](#)

Percent Identity to

E value to

Query Coverage to

[Filter](#) [Reset](#)

Descriptions | [Graphic Summary](#) | [Alignments](#) | [Taxonomy](#)

Sequences producing significant alignments [Download](#) ▾ [Manage Columns](#) ▾ Show ▾ ⓘ

select all 4 sequences selected [GenBank](#) [Graphics](#) [Distance tree of results](#)

Description	Max Score	Total Score	Query Cover	E value	Per. Ident	Accession
<input checked="" type="checkbox"/> Homo sapiens BAC clone RP11-162K6 from 4 complete sequence	279	279	100%	2e-71	100.00%	AC097711.2
<input checked="" type="checkbox"/> Canis lupus familiaris breed Labrador retriever chromosome 32a	274	274	100%	9e-70	99.34%	CP050598.1
<input checked="" type="checkbox"/> Canis lupus familiaris breed Labrador retriever chromosome 32b	274	274	100%	9e-70	99.34%	CP050634.1
<input checked="" type="checkbox"/> Mus musculus BAC clone RP24-204J10 from 5 complete sequence	252	252	100%	4e-63	96.69%	AC121929.2

Figure 23: Unique, fully-matched 100% read from Homo Sapiens is recovered from the dataset SRX7724752.

[← Edit Search](#) Save Search Search Summary ▾

Job Title **ref[NW_015351248.1]**

RID [KJ435D3801R](#) Search expires on 08-17 18:54 pm [Download All](#) ▾

Program **BLASTN** [Citation](#) ▾

Database **SRA** [See details](#) ▾

Query ID [NW_015351248.1](#)

Description **Marmota marmota marmota unplaced genomic scaffold, ma...**

Molecule type **dna**

Query Length **19578880**

Other reports [Distance tree of results](#) [MSA viewer](#) ?

[How to read this report?](#) [BLAST Help Videos](#) [Back to Traditional Results Page](#)

Filter Results

Organism *only top 20 will appear* exclude

Type common name, binomial, taxid or group name

[+ Add organism](#)

Percent Identity **E value** **Query Coverage**

to to to

[Filter](#) [Reset](#)

Descriptions Graphic Summary Alignments

Sequences producing significant alignments Download ▾ Manage Columns ▾ Show ?

select all 100 sequences selected [Graphics](#) [Distance tree of results](#)

Description	Max Score	Total Score	Query Cover	E value	Per. Ident	Accession
<input checked="" type="checkbox"/> SRX7724752	279	279	0%	2e-68	100.00%	SRA:SRR11085797.70411148.2
<input checked="" type="checkbox"/> SRX7724752	278	278	0%	9e-68	100.00%	SRA:SRR11085797.4666606.2
<input checked="" type="checkbox"/> SRX7724752	276	276	0%	3e-67	100.00%	SRA:SRR11085797.8742622.2

[← Edit Search](#) Save Search Search Summary ▾

Job Title **2 sequences [gnl|SRA|SRR11085797.10431565.1...**

RID [KJ3PSXP014](#) Search expires on 08-17 18:47 pm [Download All](#) ▾

Results for ▾

Program **BLASTN** [Citation](#) ▾

Database **nt** [See details](#) ▾

Query ID **1:c|Query_51896**

Description **gnl|SRA|SRR11085797.10431565.1 10431565 (Biological)**

Molecule type **dna**

Query Length **151**

Other reports [Distance tree of results](#) ?

[How to read this report?](#) [BLAST Help Videos](#) [Back to Traditional Results Page](#)

Filter Results

Organism *only top 20 will appear* exclude

Type common name, binomial, taxid or group name

[+ Add organism](#)

Percent Identity **E value** **Query Coverage**

to to to

[Filter](#) [Reset](#)

Descriptions Graphic Summary Alignments Taxonomy

Sequences producing significant alignments Download ▾ Manage Columns ▾ Show ?

select all 45 sequences selected [GenBank](#) [Graphics](#) [Distance tree of results](#)

Description	Max Score	Total Score	Query Cover	E value	Per. Ident	Accession
<input checked="" type="checkbox"/> Canis lupus familiaris breed Labrador retriever chromosome 32a	279	279	100%	2e-71	100.00%	CP050598.1
<input checked="" type="checkbox"/> Canis lupus familiaris breed Labrador retriever chromosome 32b	279	279	100%	2e-71	100.00%	CP050634.1
<input checked="" type="checkbox"/> Homo sapiens VISTA enhancer hs712 (LOC110120752) on chromosome 4	279	279	100%	2e-71	100.00%	HG_053377.1
<input checked="" type="checkbox"/> Homo sapiens BAC clone RP11-476H13 from 4, complete sequence	279	279	100%	2e-71	100.00%	AC024192.6
<input checked="" type="checkbox"/> Aquila chrysaetos chrysaetos genome assembly chromosome:1	274	274	100%	9e-70	99.34%	LR606181.1
<input checked="" type="checkbox"/> Streptopelia turtur genome assembly chromosome:4	274	274	100%	9e-70	99.34%	LR594554.1
<input checked="" type="checkbox"/> PREDICTED: Cyanistes caeruleus uncharacterized LOC111928864 (LOC111928864)_ncRNA	274	274	100%	9e-70	99.34%	XR_002864354.1
<input checked="" type="checkbox"/> Apteryx australis mantelli genome assembly AptMant0_scaffold scaffold564	274	274	100%	9e-70	99.34%	LK065221.1
<input checked="" type="checkbox"/> Anas platyrhynchos genome assembly chromosome:4	274	274	100%	9e-70	99.34%	LS423614.1

Job Title **2 sequences (gnl|SRA|SRR11085797.4967337.1...**

RID [KJ8SKF2E014](#) Search expires on 08-17 20:14 pm [Download All](#) ▾

Results for ▾

Program BLASTN [Citation](#) ▾

Database nt [See details](#) ▾

Query ID lcl|Query_37435

Description gnl|SRA|SRR11085797.4967337.2 4967337 (Biological)

Molecule type dna

Query Length 151

Other reports [Distance tree of results](#) ⓘ

Filter Results

Organism *only top 20 will appear* exclude

[+ Add organism](#)

Percent Identity to E value to Query Coverage to

[Filter](#) [Reset](#)

Descriptions | Graphic Summary | Alignments | Taxonomy

Sequences producing significant alignments Download ▾ Manage Columns ▾ Show 100 ▾ ⓘ

select all 58 sequences selected

Description	Max Score	Total Score	Query Cover	E value	Per. Ident	Accession
<input checked="" type="checkbox"/> Canis lupus familiaris breed Labrador retriever chromosome 32a	279	279	100%	2e-71	100.00%	CP050598.1
<input checked="" type="checkbox"/> Canis lupus familiaris breed Labrador retriever chromosome 32b	279	279	100%	2e-71	100.00%	CP050634.1
<input checked="" type="checkbox"/> Rhesus Macaque BAC CH250-499F11.1 complete sequence	274	274	100%	9e-70	99.34%	AC204215.5
<input checked="" type="checkbox"/> Homo sapiens BAC clone RP11-678H22 from 4 complete sequence	274	274	100%	9e-70	99.34%	AC096766.3
<input checked="" type="checkbox"/> Mus musculus chromosome 5 clone RP24-315H14 complete sequence	263	263	100%	2e-66	98.01%	AC105976.13
<input checked="" type="checkbox"/> Chrysemys picta isolate 4965chr ultra conserved element locus chr4_11164 genomic sequence	257	257	100%	9e-65	97.35%	JQ873778.1
<input checked="" type="checkbox"/> Alligator mississippiensis isolate 333all ultra conserved element locus chr4_11164 genomic sequence	257	257	100%	9e-65	97.35%	JQ869146.1
<input checked="" type="checkbox"/> Apteryx australis mantelli genome assembly AptMant0_scaffold scaffold564	241	241	100%	9e-60	95.36%	LK065221.1
<input checked="" type="checkbox"/> Erithacus rubecula genome assembly chromosome_5	231	231	82%	6e-57	100.00%	LR812107.1
<input checked="" type="checkbox"/> Streptopelia turtur genome assembly chromosome_4	231	231	82%	6e-57	100.00%	LR594554.1
<input checked="" type="checkbox"/> Aquila chrysaetos chrysaetos genome assembly chromosome_1	226	226	82%	3e-55	99.20%	LR606181.1

Figure. 24: Marmota Marmota genetic scaffold assemblies returned significant amount of 100% full-length matched reads that were sometimes also found in Homo Sapiens and Canis Lupus Famillaris.

Reads (separated)

>gnl|SRA|SRR11085797.6341838.1 6341838 (Biological)
 CGAGACCATCCTGGCTAACACGGTGAACCCCGTCTCTACTAAAAATACAAAAAATTAGC
 CGGGCGTGATGGCGGGCGCCTGTAGTCCCAGCTACTCGGGAGGCTGAGGCAGGAGAAATGG
 CGTGAACCCGGGAGGCGGAGCNTGCAGTG

>gnl|SRA|SRR11085797.6341838.2 6341838 (Biological)
 CTCACTGCAAGCTCCGCCGCCGGGTTCCAGCCATTCTCCTGCCTCAGCCTCCCGAGTAG
 CTGGGACTACAGGC GCCCGCCATCACGCCCGGCTAATTTTGTATTTTGTAGTAGAGACC
 GGGTTTCCCGTGTAGCCAGGATGGTCTCG

Description gnl|SRA|SRR11085797.6341838.2 6341838 (Biological)

Molecule type dna

Query Length 151

Other reports [Distance tree of results](#) ⓘ

Sequences producing significant alignments Download ▾ Manage Columns ▾ Show 100 ▾ ⓘ

select all 100 sequences selected

Description	Max Score	Total Score	Query Cover	E value	Per. Ident	Accession
<input checked="" type="checkbox"/> Pongo abelii chromosome 10 clone CH276-326B4 complete sequence	278	1689	100%	7e-71	100.00%	AC270645.1
<input checked="" type="checkbox"/> Pongo abelii chromosome 10 clone CH276-12G11 complete sequence	278	1379	100%	7e-71	100.00%	AC270533.1
<input checked="" type="checkbox"/> Pongo abelii chromosome 10 clone CH276-5H9 complete sequence	278	1253	100%	7e-71	100.00%	AC270518.1
<input checked="" type="checkbox"/> Homo sapiens beta-1.3-galactosyltransferase 1 (B3GALT1) mRNA	274	274	100%	9e-70	99.34%	NM_020981.4
<input checked="" type="checkbox"/> Homo sapiens chromosome 1 clone VMRC53-455P10 complete sequence	274	3094	100%	9e-70	99.34%	AC278561.1

Figure.25a: 100% full-length matched reads to Hominid(Pongo Abelii) genomic DNA.

<input checked="" type="checkbox"/>	Human endogenous retrovirus H HERV-H/env60 proviral copy clone 734E12	252	252	100%	4e-63	96.69%	AJ289710.2
<input checked="" type="checkbox"/>	Synthetic human HSC3N1 Alu sequence	252	252	100%	4e-63	96.69%	U02043.1
<input checked="" type="checkbox"/>	Synthetic construct complete sequence	250	3635	100%	1e-62	96.69%	JN255744.1
<input checked="" type="checkbox"/>	Human artificial chromosome vector 21HAC4 DNA isolated from the long arm clone YAC/BAC#26-2	250	1964	100%	1e-62	96.69%	AB553834.1
<input checked="" type="checkbox"/>	Human ORFeome Gateway entry vector pENTR223-MGC2752 complete sequence	246	246	100%	2e-61	96.05%	L7735229.1
<input checked="" type="checkbox"/>	Expression vector pUMLIEP DNA complete sequence	246	246	99%	2e-61	96.05%	LC175306.1
<input checked="" type="checkbox"/>	Synthetic construct Homo sapiens clone ccsbBroadEn_10246 MGC2752 gene encodes complete protein	246	246	100%	2e-61	96.05%	KJ900852.1
<input checked="" type="checkbox"/>	HIV-1 isolate HK_JIDLNBL_S071 from Switzerland nonfunctional gag protein (gag) gene complete sequence and nonfunction	244	1072	100%	7e-61	96.00%	MT154980.1
<input checked="" type="checkbox"/>	Cloning vector pSuper_7SL_AlucAA 7SL enhancer and AluYa5 repeat element sequence	241	241	100%	9e-60	95.36%	EU092258.1
<input checked="" type="checkbox"/>	Cloning vector pSuper_7SL_AlucA 7SL enhancer and AluYa5 repeat element sequence	241	241	100%	9e-60	95.36%	EU092257.1
<input checked="" type="checkbox"/>	Synthetic construct clone AluAU SRP promoter region and Alu repeat element sequence	241	241	100%	9e-60	95.36%	AF458115.1
<input checked="" type="checkbox"/>	Synthetic construct clone AluWD SRP promoter region and Alu repeat element sequence	241	241	100%	9e-60	95.36%	AF458112.1
<input checked="" type="checkbox"/>	Synthetic construct clone AluT253 SRP promoter region and Alu repeat element sequence	241	241	100%	9e-60	95.36%	AF458107.1
<input checked="" type="checkbox"/>	Synthetic construct clone AluA SRP promoter region and Alu repeat element sequence	241	241	100%	9e-60	95.36%	AF458106.1
<input checked="" type="checkbox"/>	Desmodus rotundus isolate DRU21DN04 contig68764 whole genome shotgun sequence	108	216	63%	2e-20	87.23%	PEHR01068758.1
<input checked="" type="checkbox"/>	Myotis lucifugus cont2.6286 whole genome shotgun sequence	108	108	55%	2e-20	90.36%	AAPE02006287.1
<input checked="" type="checkbox"/>	Artibeus jamaicensis isolate US092 ArtJam_scaffold_27825 whole genome shotgun sequence	104	104	51%	2e-19	90.91%	PVKR01013927.1
<input checked="" type="checkbox"/>	Macrotus californicus isolate US035 MacCal_line_566643 whole genome shotgun sequence	102	102	51%	9e-19	90.79%	VMDR010283404.1
<input checked="" type="checkbox"/>	Anoura caudifer isolate US021 Anocau_scaffold_336054 whole genome shotgun sequence	102	102	61%	9e-19	86.96%	PVKU01163203.1
<input checked="" type="checkbox"/>	Anoura caudifer isolate US021 Anocau_scaffold_250162 whole genome shotgun sequence	102	102	61%	9e-19	86.96%	PVKU01121529.1
<input checked="" type="checkbox"/>	Anoura caudifer isolate US021 Anocau_scaffold_157416 whole genome shotgun sequence	102	102	61%	9e-19	86.96%	PVKU01078866.1
<input checked="" type="checkbox"/>	Anoura caudifer isolate US021 Anocau_scaffold_136788 whole genome shotgun sequence	102	102	61%	9e-19	86.96%	PVKU01068554.1
<input checked="" type="checkbox"/>	Anoura caudifer isolate US021 Anocau_scaffold_6229 whole genome shotgun sequence	102	102	51%	9e-19	90.79%	PVKU01003121.1
<input checked="" type="checkbox"/>	Anoura caudifer isolate US021 Anocau_scaffold_1146 whole genome shotgun sequence	102	102	71%	9e-19	84.26%	PVKU01000576.1
<input checked="" type="checkbox"/>	Artibeus jamaicensis isolate US092 ArtJam_scaffold_590481 whole genome shotgun sequence	102	102	51%	9e-19	90.79%	PVKR01295479.1
<input checked="" type="checkbox"/>	Artibeus jamaicensis isolate US092 ArtJam_scaffold_272373 whole genome shotgun sequence	102	102	51%	9e-19	90.79%	PVKR01136397.1
<input checked="" type="checkbox"/>	Rhinolophus ferrumequinum isolate MPI-CBG mRhiFer1_000055F_070_arrow_arrow whole genome shotgun sequence	101	101	51%	8e-19	88.46%	RXPD01003063.1
<input checked="" type="checkbox"/>	Rhinolophus ferrumequinum isolate mRhiFer1_scaffold_m29_p_7 whole genome shotgun sequence	101	151	51%	8e-19	88.46%	JACAGC010000007.1
<input checked="" type="checkbox"/>	Rhinolophus ferrumequinum RF_contig_107525 whole genome shotgun sequence	101	101	51%	8e-19	88.46%	AWHA01101756.1
<input checked="" type="checkbox"/>	Rhinolophus ferrumequinum isolate US033 RhiFer_flattened_line_8799 whole genome shotgun sequence	97.8	186	50%	1e-17	88.16%	VMDN01004402.1
<input checked="" type="checkbox"/>	Rhinolophus ferrumequinum isolate MPI-CBG mRhiFer1_000061F_062_arrow_arrow whole genome shotgun sequence	97.8	186	50%	1e-17	88.16%	RXPD01001710.1
<input checked="" type="checkbox"/>	Rhinolophus ferrumequinum isolate MPI-CBG mRhiFer1_chromosome_6 whole genome shotgun sequence	97.8	309	50%	1e-17	88.16%	RXPC01000086.1
<input checked="" type="checkbox"/>	Rhinolophus ferrumequinum isolate mRhiFer1_scaffold_m29_p_8 whole genome shotgun sequence	97.8	309	50%	1e-17	88.16%	JACAGC010000008.1
<input checked="" type="checkbox"/>	Rhinolophus ferrumequinum isolate MPI-CBG mRhiFer1_000003F_100_arrow_arrow whole genome shotgun sequence	93.3	93.3	49%	1e-16	88.00%	RXPD01006157.1
<input checked="" type="checkbox"/>	Rhinolophus ferrumequinum isolate mRhiFer1_scaffold_m29_p_4 whole genome shotgun sequence	93.3	93.3	49%	1e-16	88.00%	JACAGC010000004.1
<input checked="" type="checkbox"/>	Rhinolophus ferrumequinum isolate US033 RhiFer_flattened_line_6166 whole genome shotgun sequence	90.6	90.6	44%	1e-15	89.55%	VMDN01003085.1
<input checked="" type="checkbox"/>	Rhinolophus ferrumequinum isolate MPI-CBG mRhiFer1_000061F_073_arrow_arrow whole genome shotgun sequence	90.6	90.6	44%	1e-15	89.55%	RXPD01006658.1

Fig.25b: BLAST search of this sequence revealed it to be a Homo Sapiens endogenous Retrovirus most similar to HIV-1, and is not found in any known bat genomic assemblies. This sequence is also found in several cloning vectors for mammalian DNA. Significance of these sequences are currently unknown.

SRX7724752 contained Traces of confirmed contamination from other organisms, in particularly that of order Carnivora, Rodentia and Homo Sapiens. As such DNA contamination mostly happen during extensive manipulation of samples in the labs, This indicate that SRX7724752 Contained traces of laboratory manipulation, including Canis Lupus Famillaris DNA contamination which could not have been present in a fecal sample of a bat, even assuming normal lab manipulation for sequencing purposes.

This indicate the sample may have been subjected to in-vitro manipulation.

No evidence of methodological reasons for the generation of anomalies in SRX7724752

In Order to test whether a specific sequencing technique was used for the sequencing of SRX7724752 which may have generated the anomalies observed above, we decided to use the sequencing depth of the Coronaviruses within SRX7724752 and compare it against another set of

mNGS sequencing data of identical sample, origin, institute and submitted at the same date, located in [PRJNA606159](https://www.ncbi.nlm.nih.gov/bioproject/606159).

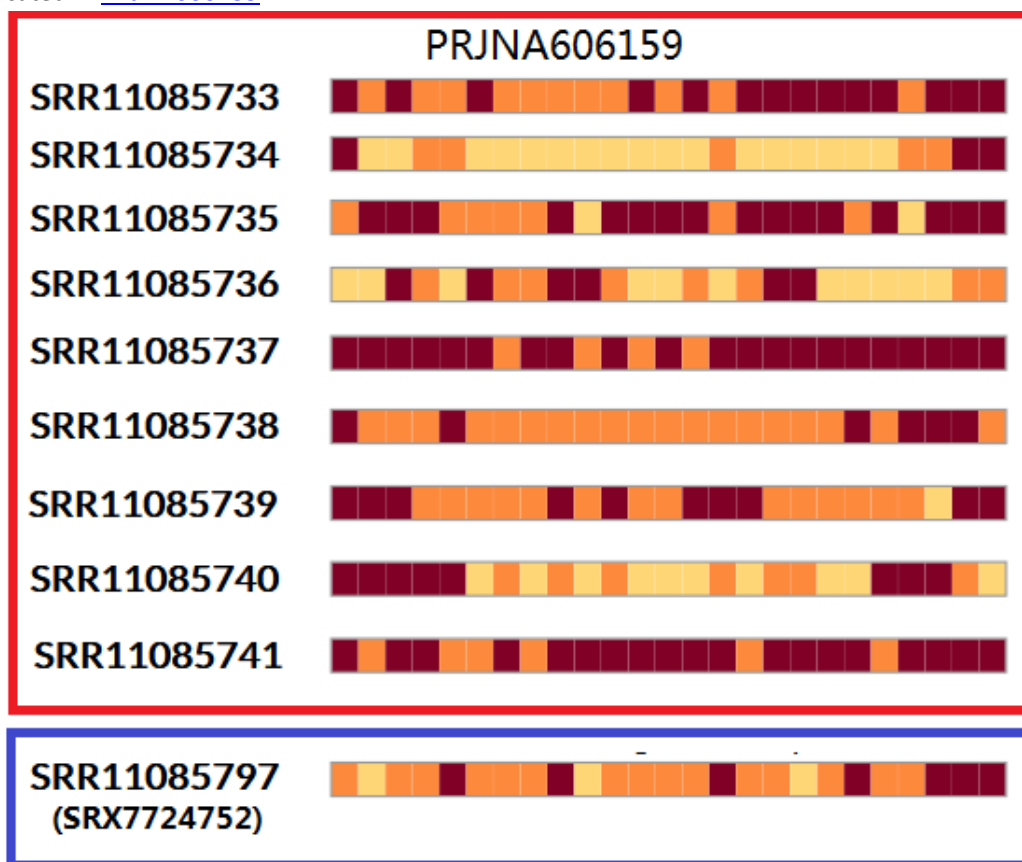


Fig. 26a: the Coverage map of Coronaviridae within the datasets located in PRJNA606159, compared against SRR11085797.

We generated the sequencing depth Heatmap [8] of all datasets located within PRJNA606159, and the sequencing depth pattern of the Coronavirus reads within such dataset does not show any statistical differences from that of SRR11085797.

[SRX7724696](https://www.ncbi.nlm.nih.gov/bioproject/606159): RNA-Seq of *Hipposideros larvatus*: Anal swab
1 ILLUMINA (Illumina HiSeq 3000) run: 13.5M spots, 3.9G bases, 1.8Gb downloads

Design: Total RNA was extracted from bronchoalveolar lavage fluid using the QIAamp Viral RNA Mini Kit following the manufacturers instructions. An RNA library was then constructed using the TruSeq Stranded mRNA Library Preparation Kit (Illumina, USA). Paired-end (150 bp) sequencing of the RNA library was performed on the HiSeq 3000 platform (Illumina).

Submitted by: Wuhan Institute of Virology, Chinese Academy of Sciences

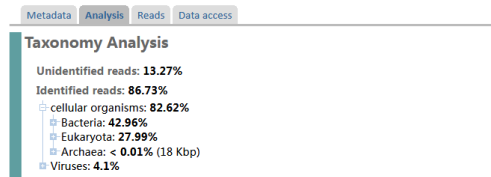
[SRX7724752](https://www.ncbi.nlm.nih.gov/bioproject/606159): RNA-Seq of *Rhinolophus affinis*: Fecal swab
1 ILLUMINA (Illumina HiSeq 3000) run: 11.6M spots, 3.3G bases, 1.7Gb downloads

Design: Total RNA was extracted from bronchoalveolar lavage fluid using the QIAamp Viral RNA Mini Kit following the manufacturers instructions. An RNA library was then constructed using the TruSeq Stranded mRNA Library Preparation Kit (Illumina, USA). Paired-end (150 bp) sequencing of the RNA library was performed on the HiSeq 3000 platform (Illumina).

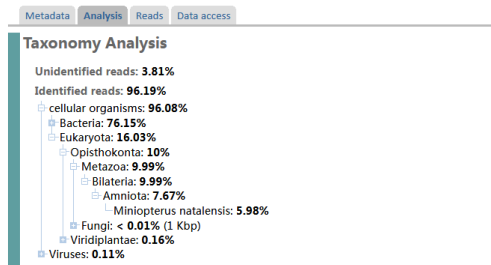
Submitted by: Wuhan Institute of Virology, Chinese Academy of Sciences

Fig.26b: the experimental design section of the datasets within PRJNA606159 is identical to that of SRX7724752.

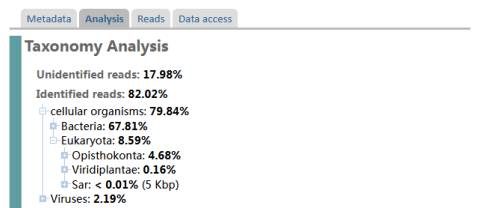
RNA-Seq of *Hipposideros larvatus*: Anal swab (SRR11085733)



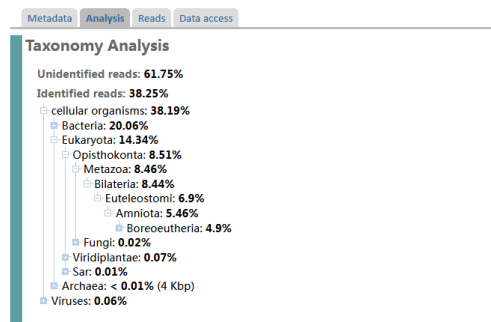
RNA-Seq of *Miniopterus schreibersii*: Anal swab (SRR11085734)



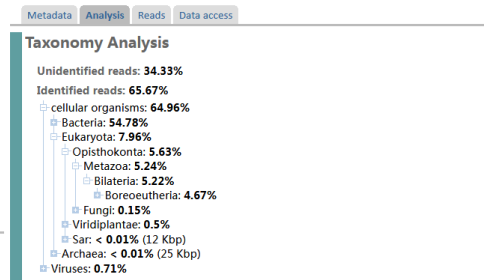
RNA-Seq of *Scotophilus kuhlii*: Anal swab (SRR11085737)



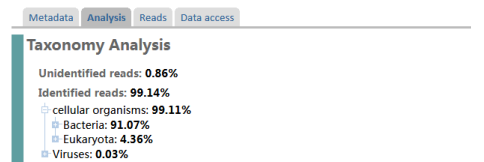
RNA-Seq of *Tylonycteris pachypus*: Anal swab (SRR11085739)



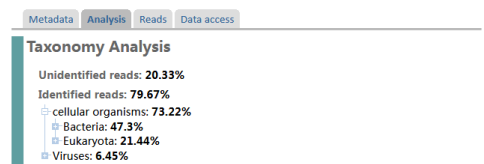
RNA-Seq of *Hipposideros pomona*: Anal swab (SRR11085735)



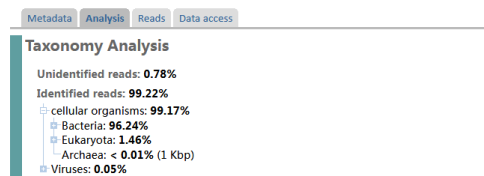
RNA-Seq of *Rhinolophus affinis*: Anal swab (SRR11085736)



RNA-Seq of *Pipistrellus abramus*: Anal swab (SRR11085738)



RNA-Seq of *Miniopterus pusillus*: Anal swab (SRR11085740)



RNA-Seq of *Rousettus aegyptiacus*: Anal swab (SRR11085741)

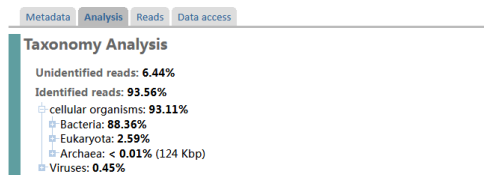


Fig.26c: No evidence of any anomalies were found within the datasets presented in PRJNA606159

We recently obtained a set of viral mNGS coverage data from a sequencing experiment that Uses PolyA enrichment for the selection of sequences [9].

Despite being isolated from the total RNA of freshly dissected and cleaned Bee Tissue samples, these PolyA enriched datasets displayed a heavy bias toward the 3'-end for all viral genomes that contained a polyA tail, and did not obtain any coverage past 8000nt to the 3'-end of such viral genomes. This is consistent with the fact that viral genomic RNA obtained from samples, even when freshly prepared, will always suffer from numerous RNA strand breaks, and therefore will be heavily biased toward the 3'-end as the enrichment process would have kept mostly the RNA that contained an intact polyA tail. As Coronaviruses have a PolyA tail, this is in sharp contrast to that found in SRX7724752, which does not show signs of such bias.

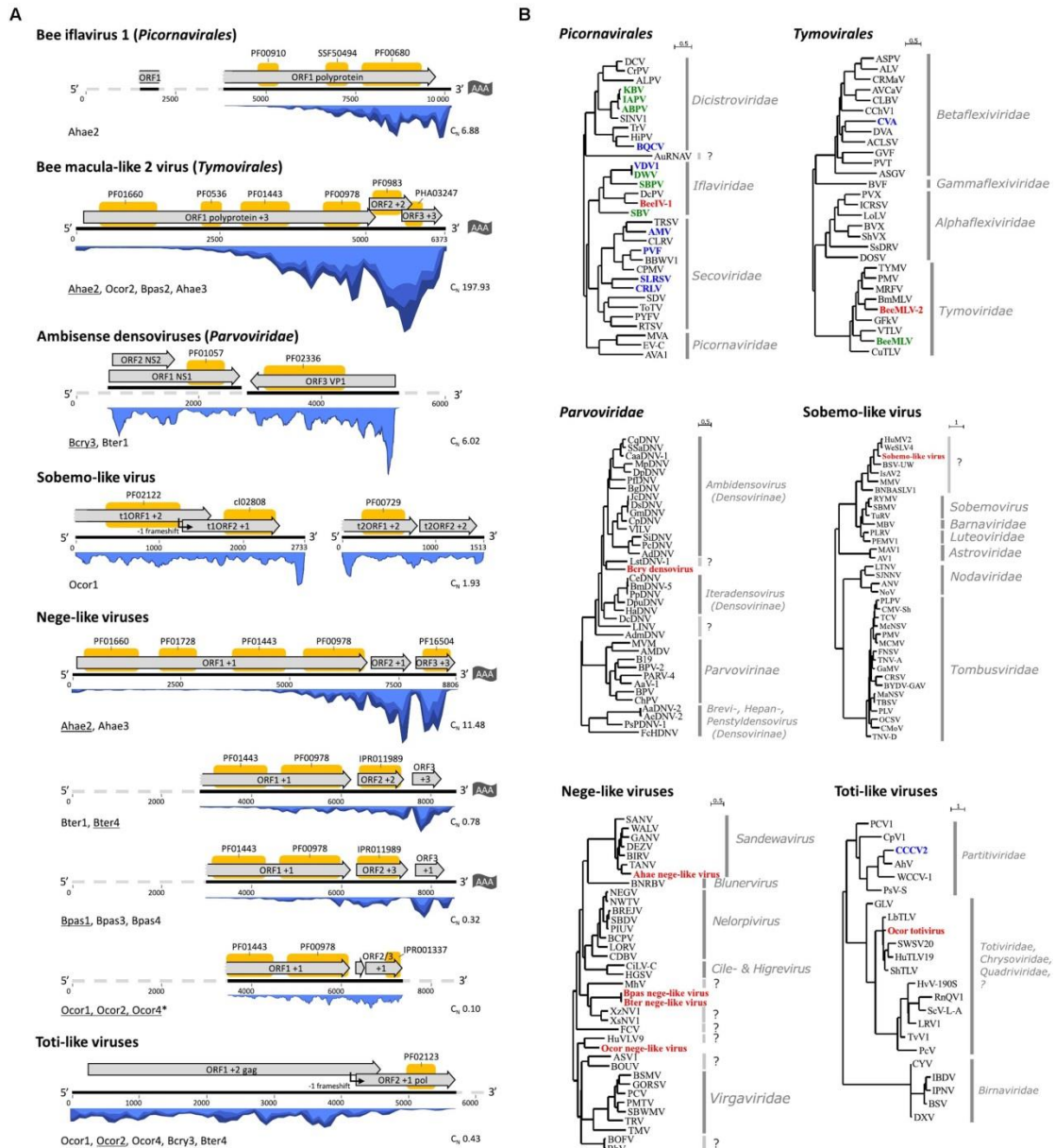


Figure 2 from [9]. A clear bias toward the 3'-end of RNA viral families that contained a polyA tail, was noticed.

The anomalies in SRX7724752 is associated with the absence of RNA viruses.

In order to further analyze the implications of the observed anomalies in SRX7724752, we performed a Keyword search on NCBI SRA using the Keyword "Bat feces" and "Bat fecal". We did not find any evidence of an RNA virus (Riboviria) within any of the returned datasets that contained less than 2.5% bacteria in total cellular organisms that can be confirmed by BLAST.

Description	Phaseolus vulgaris endornavirus 1 isolate PvEV-1_Brazil poly ...
Molecule type	nucleic acid
Query Length	14072
Other reports	?

! No significant similarity found. For reasons why, [click here](#)

Figure 27: an example of a TRACE result that does not actually exist when BLASTed against the reference sequences of said virus.

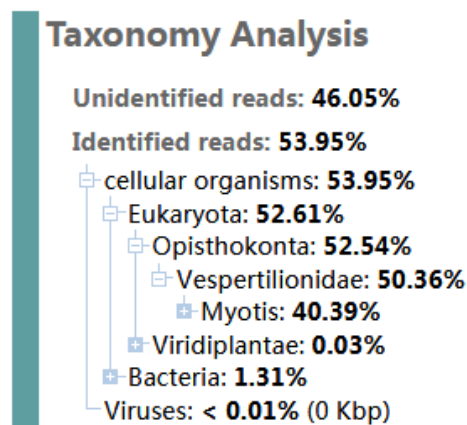


Figure 28a: an example of a bacteria-depleted dataset. An absence of Riboviria reads was noted.

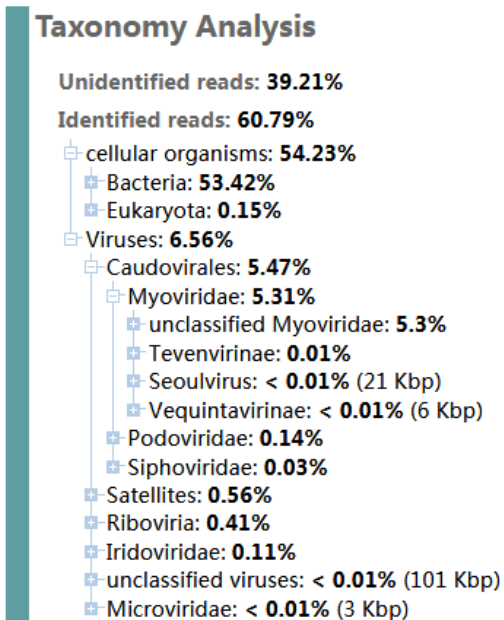


Figure 28b: in contrast, Riboviria reads are found only in datasets that contained a significant amount of bacteria.

In addition, We found only 1 dataset that contained any significant levels of a Telomere-like repeat sequence. However, this dataset does not contain any evidence of an RNA virus(Riboviria).

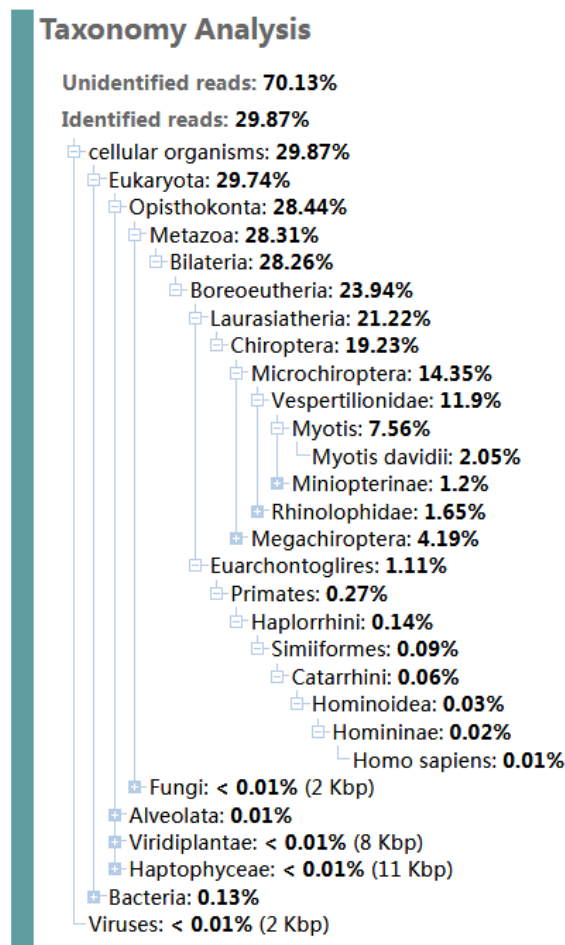


Figure 29: the only dataset with significant level of Telomere-like repeats (2%). There are no evidence of Riboviria(RNA viruses) within this dataset.

Signature of likely attenuation of the RaTG13 RBD.

The RaTG13 RBD have reduced binding affinity to ACE2 compared to other viruses of the same clade.

Recently, a publication which tested the binding affinity and infection efficiency of RaTG13 S to human ACE2[10] have been published, which suggest that unlike the other RBDs within this clade (namely SARS-CoV-2 and pCoV_GX), RaTG13 can not bind to human ACE2 efficiently, and is incapable of entering cells through ACE2 that is expressed at physiological levels.

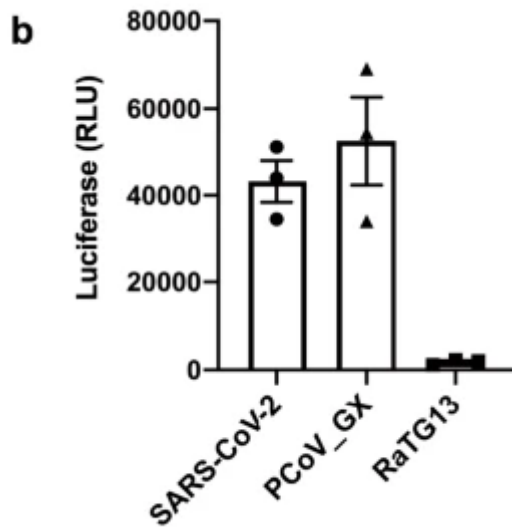
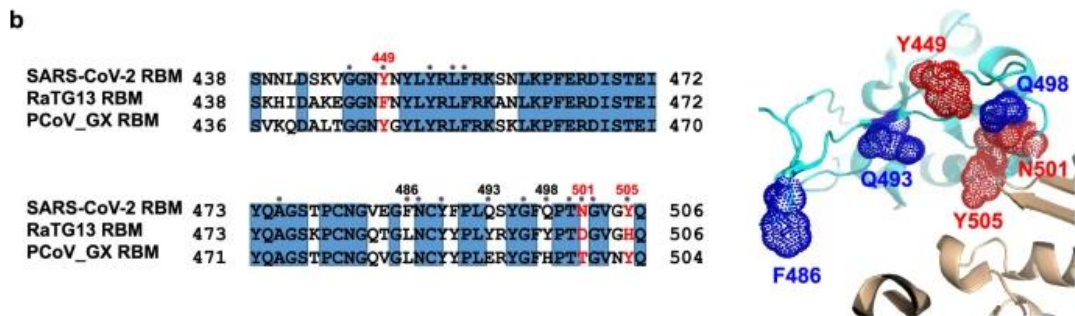
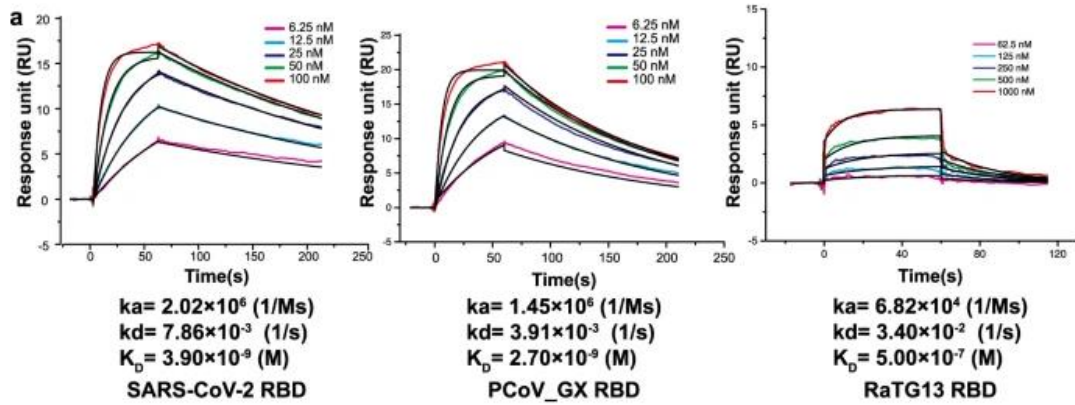


Fig.5a and 6b from [10]: RaTG13 RBD bound to human ACE2 very inefficiently, and did not show entry into hACE2-HEK293T cells at physiological level of ACE2 expression.

Initially considered as evidence of “bat specificity” for RaTG13, An recent test [11] did not find any higher binding affinity of the RaTG13 RBD to R.affinis ACE2 than to human ACE2—in fact, both the flow cytometry data and the pseudovirus entry data into HEK293T with Overexpressed ACE2 suggest a binding affinity of RaTG13 RBD to R.affinis ACE2 that is slightly lower than that of RaTG13 RBD to human ACE2.

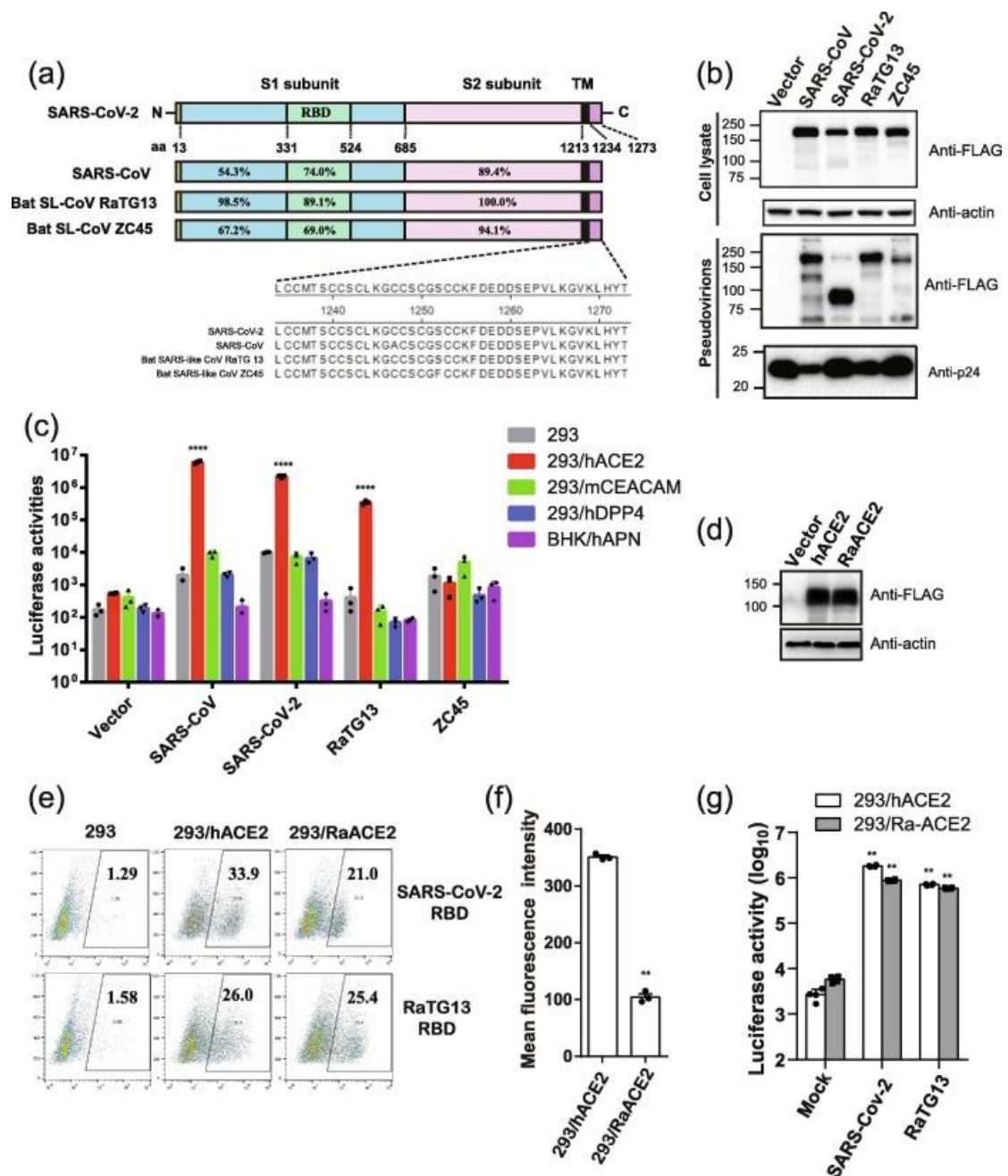


Fig.5 from [11]: d: The overexpression level for human and R.affinis ACE2 on the HEK293T cells are the same. e: The binding affinity of RaTG13 RBD-Fc on R.affinis ACE2(Lower Right) is slightly lower than the binding affinity of RaTG13 RBD-Fc on human ACE2(Lower Middle), and is significantly lower than the binding affinity of SARS-CoV-2 RBD to human ACE2(Upper middle). g: Pseudovirus entry assay using Lentivirus on HEK293T with Overexpressed ACE2 show that SARS-CoV-2-hACE2 > SARS-CoV-2-R.affinis ACE2 > RaTG13-hACE2 > RaTG13-R.affinis ACE2 by pseudovirus entry efficiency.

A multiple alignment of the RaTG13 Spike protein RBD to other Sarbecovirus Spike protein RBDs quickly revealed two specific residues—T403 and D501—that were never found in other Sarbecoviruses. In addition, H505 is found to be absent in all previous R.affinis infecting Sarbecoviruses.

1 10 20 30 40 50 60 70 80 90 100 110 121

QHR63300.2:400-520
620F_A:431-551
704R_A:400-520
QJE37811.1:96-216
QRV71349.1:181-201
QNS17503.1:118-238
QRV71345.1:181-201
QRV71340.1:181-201
7L7F_E:90-210
QK172177.1:404-524
Q0667583.1:410-530
Q1055887.1:400-520
Q0667582.1:400-520
QJE37812.1:400-520
7E7D_A:400-520
704N_A:400-520
QLR06866.1:396-516
QLR06864.1:396-516
R06867.1:396-516
Q1055945.1:396-516
788H_A:396-516
6W1L_E:82-202
Q1A08632.1:398-517
Q1A06614.1:398-517
708R_A:398-517
Q1A08641.1:398-517
Q1044068.1:400-519
Q1A08623.1:398-515
AG248787.1:399-158
RT098205.1:387-506
RLK92457.1:387-506
AG248828.1:388-507
AG248818.1:388-507
RHK37569.1:391-510
RHK37569.1:391-510
QDF43825.1:388-507
RT098219.1:388-507
RT098231.1:388-507
386F_A:70-189
208H_C:74-193
208D_S:71-190
QK12178.1:404-523
RB727215.1:387-506
5X6R_A:374-493
5MR6_A:387-506
6N6E_A:406-525
6CRH_A:374-493
68LC_A:387-506
RC10703.1:387-506
RB072985.1:387-506
RC272093.1:387-506
RB072982.1:387-506
RAR07630.1:387-506
RAR31586.1:387-506
RC063863.1:387-506
RAR05193.1:387-506
RC272254.1:387-506
RAR01608.1:387-506
6CRV_A:374-493
RA176147.1:387-506
RC092725.1:387-506
RC272092.1:387-506
RAR07624.1:387-506
RAR13567.1:387-506
RAR57586.1:387-506
RAF43801.1:387-506
RAR073001.1:387-506
RAR23537.1:387-506
RC063860.1:387-506
RB072984.1:387-506
RB072977.1:387-506
YP_009825951.1:387-5
RFS8672.1:387-506
RC13483.1:387-506
RC271976.1:387-506
RB072979.1:387-506
RC272195.1:387-506
RB072970.1:387-506
RC271826.1:387-506
RC063854.1:387-506
RB072969.1:387-506
RC271797.1:387-506
RAF42873.1:387-506
RC272108.1:387-506
RB072988.1:387-506
RB072995.1:387-506
RC271961.1:387-506
RC063905.1:387-506
RAS00003.1:387-506
RAR6675.1:387-506
RA174874.1:387-506
RAF51227.1:387-506
70MS_E:82-201
QND76034.1:391-510
RC272122.1:387-506
RE110473.1:387-506
RBF65836.1:387-506
RA004649.1:387-506
RBF68959.1:387-506
RBF62968.1:387-506
RA004646.1:387-506
RAV91631.1:387-506
RA004662.1:387-506
RA004649.1:387-506
RAV49722.1:387-506
RA004664.1:387-506
RAV93319.1:387-506
RAV97985.1:387-506
RAV98000.1:387-506
RAV97989.1:387-506
RAV98002.1:387-506
RBF68955.1:387-506
RBF68956.1:387-506
RAV49720.1:387-506
RA004651.1:387-506
RAV97986.1:387-506
RAV97985.1:387-506
RAV49723.1:387-506
RAV97989.1:387-506
RAV49719.1:387-506
RAV97986.1:387-506

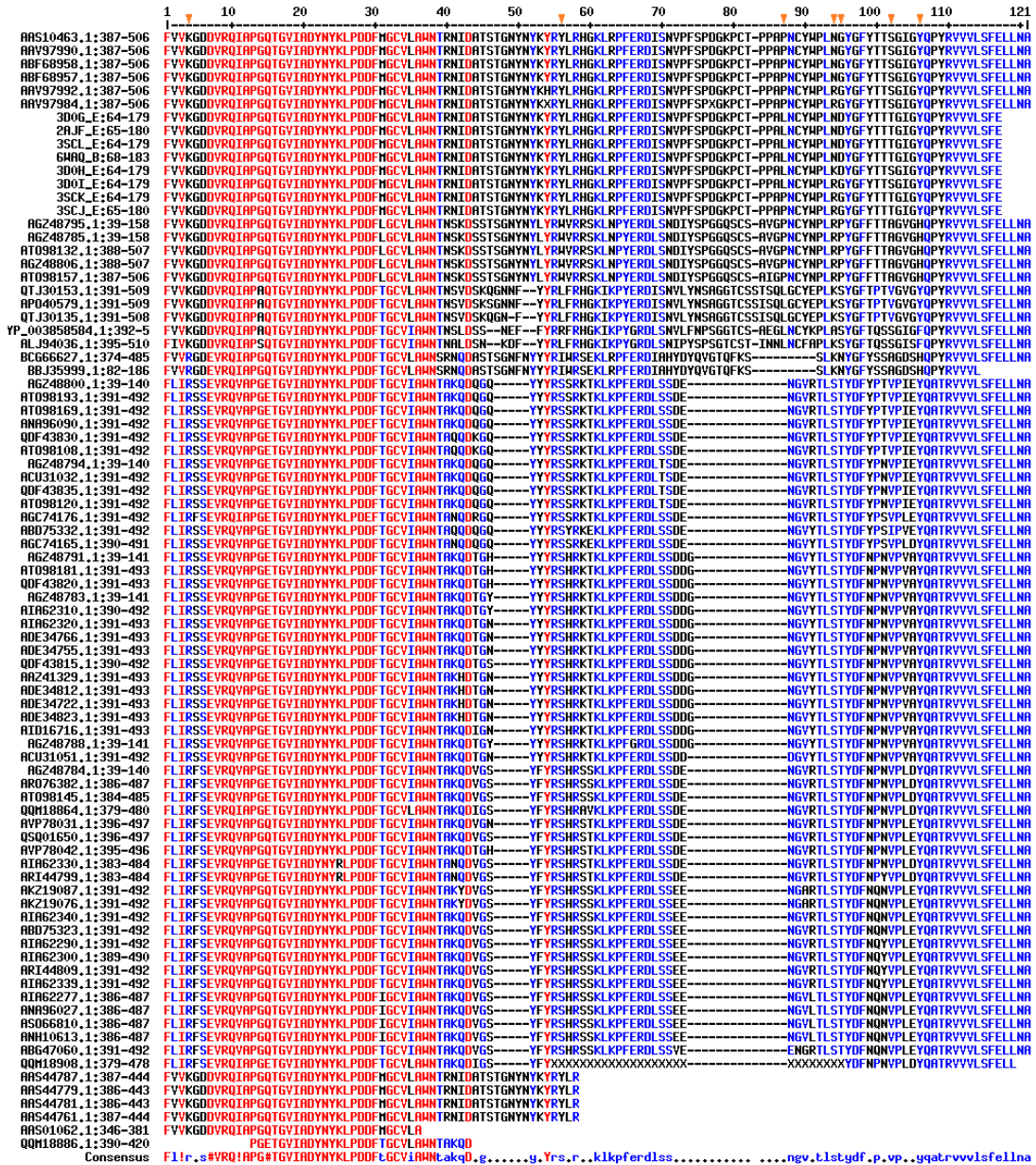


Fig.30a: multiple sequence alignment of all current known Sarbecovirus RBM sequences from NCBI. Orange arrows indicating critical residues for infection using ACE2[12][13]. Red square indicates nr and PDB sequences for the RaTG13 S.

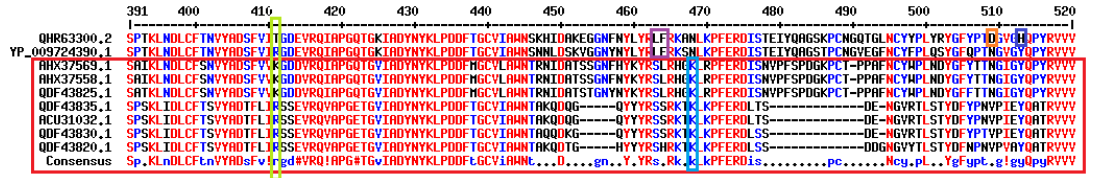


Fig.30b: multiple sequence alignment of R.affinis infecting Sarbecoviruses indicating that H505 is not found in other known Sarbecovirus sequences. Red square indicates Sarbecovirus with a host listed as “Rhinolophus Affinis”.

As these sites were found to be different in RaTG13, and since these 2 sites result in a significant change in the residue’s general properties compared to the analogous position on all other

Sarbecovirus RBD known (Basic in all other RBDs->Neural polar for R403T, Neutral in all other RBDs -> Acidic for N501D), we set to deduce their effect in the binding of the RBD to ACE2. A publication using deep mutational scanning analysis[14] suggest that Y449F, N501D and Y505H resulting in the highest reduction of binding affinity to hACE2 when applied to SARS-CoV-2.

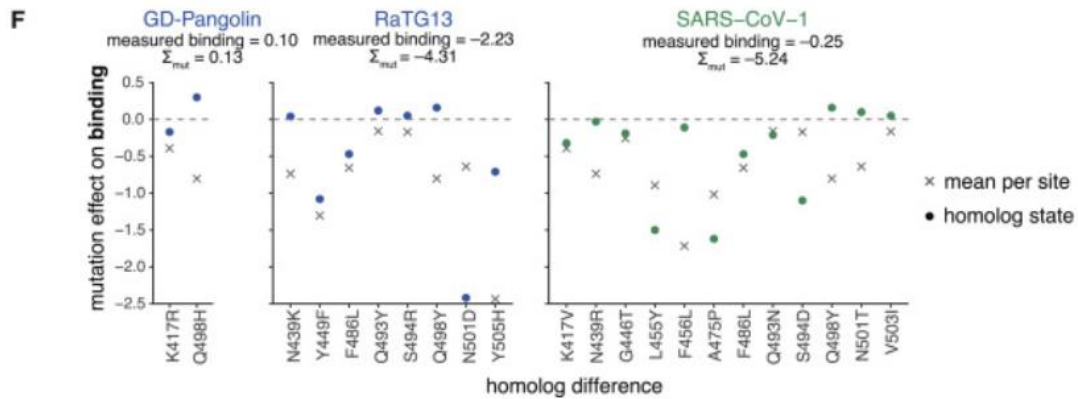


Figure 5F from [14] with different mutations from RaTG13 RBD applied to SARS-CoV-2 RBD. N501D resulted in the most severe reduction in binding affinity to ACE2, followed by Y449F and Y505H.

Using structural analysis, we discovered that the residues on ACE2 surrounding Y449, N501 and Y505 in SARS-CoV-2 are identical between Human and *R.affinis* ACE2, indicating that the reduction of binding affinity conferred by N501D, Y449F and Y505H would also cause the same reduction in binding affinity to *R.affinis* ACE2. Indeed, no sequence from *R.affinis* contained D501 or H505, implying that these 2 residues are also avoided in viruses that naturally circulating in this species, indicating that they cause a substantial reduction of viral fitness if introduced.

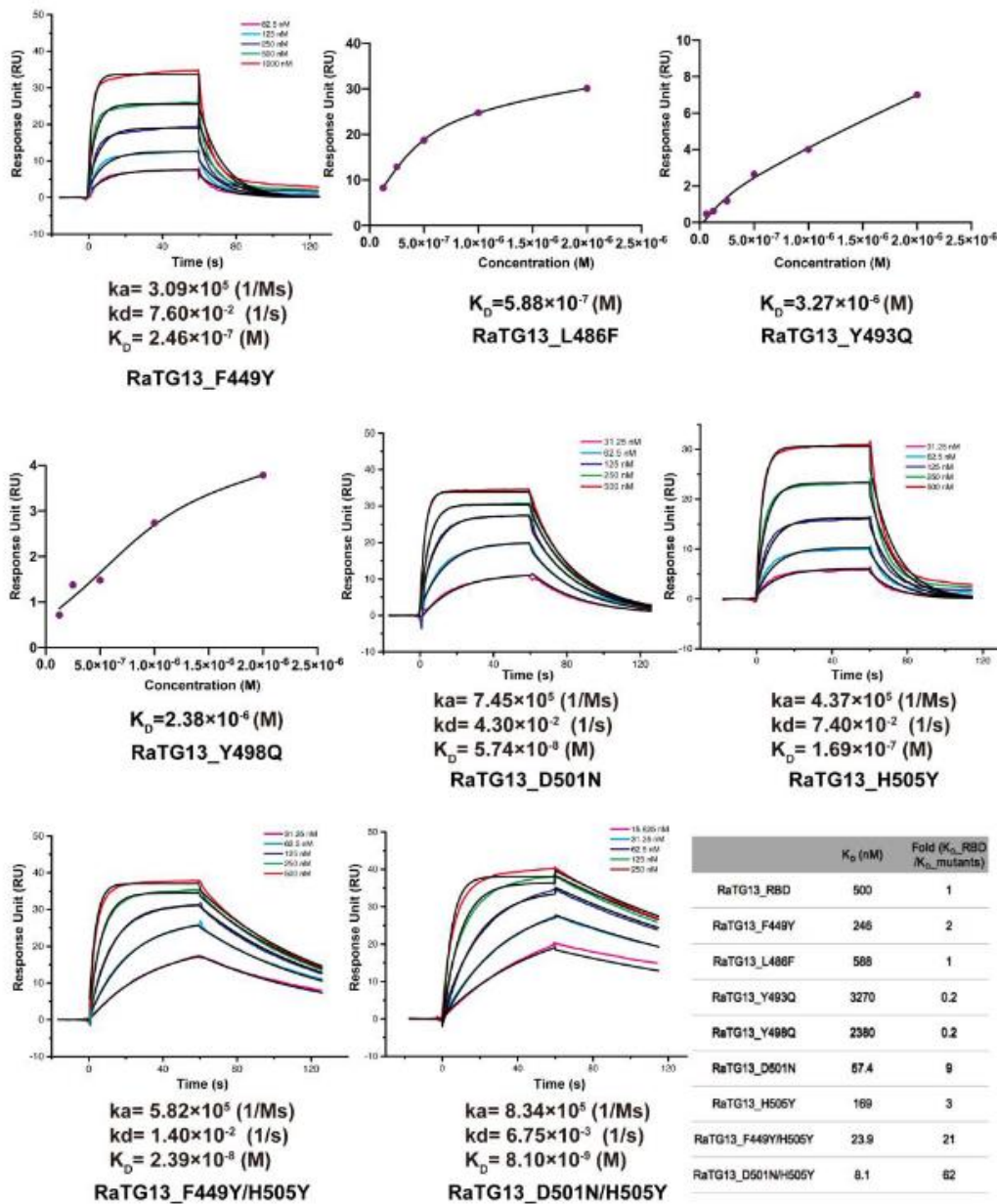


Fig. S10 from [10] denoting the effect of different amino acid substitutions on the RaTG13 RBD and their effects on binding to hACE2.

Indeed, upon mutating the position 501 and position 505 into N and Y, the consensus sequence within the R.affinis species, the binding affinity of RaTG13 RBD to ACE2 is fully restored, with an 82-fold increase compared to QHR63300.2 in term of ACE2 binding affinity. As these 2 residues interfaces with residues that were conserved between human and R.affinis ACE2, it is predicted that the same change will also improve the binding of the RaTg13 RBD to R.affinis ACE2, potentially to similar levels as SARS-CoV-2 to human ACE2.

Interestingly, the authors of [11] did not test the effect on ACE2 binding affinity of D501N or H505Y in the RaTG13 RBD, nor did they test any of the RBD mutants on R.affinis ACE2.

	1	10	20	30	40	50	60	70	80	90	100	110	120	130
NP_001358344.1	MSSSGALLLSLVYVTAAGSTIEFQAKTFLQKFNHEREDLFYQSSLASAHYNTNITFEENVQNNHAGDKHSRFLKEQSTLADHYPLQETIQNLTVKLLQLAQQSGSPVLSSEKSKRLNLTNTNSTIYSTG													
QM039244.1	MSGSSALLLSLVYVTAAGSTIEDRAKIFLDNFNHEREDLFYQSSLASAHYNTNISDEVNQNDEAGAKHSRFLYEEQSKLAKNYPLEETQVTKLQLQLQSGSPVLSSEKSKRLNLTNSTIYSTG													
Consensus	MSGSSALLLSLVYVTAAGSTIE#R#KIFLDnFNHEREDLFYQSSLASAHYNTNIS#ENVQnH#AGaKHSRFL#EQSKLAKnYPL#EIQnLpVKLQLQaLQnGSpVLSSEKSKRLN#LTn#NSTIYSTG													
NP_001358344.1	131	140	150	160	170	180	190	200	210	220	230	240	250	260
QM039244.1	KYVNPMPQECILLEPGLNEIDHNSLDYNERLHAWESHRESEVQKLRPLVEEYVLLKNEHARAHNIHEDYGDYARGDYEYVNGVGYVYSRGQLIEDVVEHTEIETKPLVEHLHAYRKLHNAYPYSISPTG													
Consensus	KYVcN#MPQECILLEPGLnEIDHnSLDyNERLHAWeSHR#E#VQKLRPLVEEYV#LLKNEHARAHNI#HEDYGDYARGDYEY#VNGVGYVY#SRGQLIEDV#VEHTEI#ETKPLVEHLHAYRKLHNA#Y#PYSISPTG													
NP_001358344.1	261	270	280	290	300	310	320	330	340	350	360	370	380	390
QM039244.1	CLPAHLGDHAGRFATNLYSLVYFQKPNIDVTDMYVQARHQAQRIFKEKEKFFVSYGLPNMTQGFHENSMLTOPGNVQKAVCHPTAHLGKGFRLIHCYKVTDDFLTAHHEHGIQDMAYRQPF													
Consensus	CLPAHLGDHAGRFATNLY#L#VYFQKPNIDVTDMY#VQARHQAQRIFKEKEKFFVSYGLPNMT#QGF#HENSMLTOPGNVQKAVCHPTAHLGKGFRLIHCYKVT#DDFLTAHHEHGIQDMAYR#QPF													
NP_001358344.1	391	400	410	420	430	440	450	460	470	480	490	500	510	520
QM039244.1	LLLRNGANEAFHEAYGEIHSLSAATPKHLKSTIGLLSPDFQEDNETEIFLFLKQALIVGTLPTFTYMLEKARHMFVKGEPKDOAHKKHMEHREIVGVYVPEVPHDQETPCOPASLHVSNDSYFIRYRTIL													
Consensus	LLLRNGANEAFHEAYGEI#HSL#SAATPKHLK#s#iGLLSPDF#q#EDNETEIFLFLKQALnIVGTLPTFTYMLEKARHMF#V#GEPK#DOAHKKHMEH#R#i#VGVYVPEVPHDQETPCOPASLHV#SNDSYFIRYRTI#i													
NP_001358344.1	521	530	540	550	560	570	580	590	600	610	620	630	640	650
QM039244.1	YDFQFQALCQAARKHEGPLHKDISNSTEAGKLFNMLRLGKSEPTLALLENVYVGRKNNHVRPLLYFEPLFTHLKDQNKSFVGHSTDMSPYADQSIVRISLKSALGDKAYEANDNEHYLFRSSVAYA													
Consensus	YDFQF#QALCQAARKHEGPLHKDISNST#AGqK#Lh#MLR#L#GKS#PTIL#L#e#!Ydar#H#V#R#PLLYFEPL#THL#q#Qn#n#S#VGHnTDMSPY#ADQSIVRISLKSALG#KAYEANDNEHYLFRSSVAYA													
NP_001358344.1	651	660	670	680	690	700	710	720	730	740	750	760	770	780
QM039244.1	HRQYFLKVKKQNILFGEDVRYANLKPRISFNFFVYTPKNVSDIIPRTEVEKAIHRSRINDAFRLDONSLEFLGIQPTLGPVPPVSTHLIVFGVGHVIVYGVVLIITGIRDRKKNKARSGENP													
Consensus	HR#YFLK#KQNI#LFGEDVRYANLKPRISFN#FFVYTPKNVSDIIPRTEVEKAIHRSRINDAFRLDONSLEFLGIQPTLGPVPPV#STHLIVFGVGHVIVYGVVLIITGIRDRKK#NKARSGENP													
NP_001358344.1	781	790	800	805										
QM039244.1	YASIDISKGENNPGFQNTDDVQTSF													
Consensus	Y#S#I#i#n#KGENNPGFQ#n#DDVQTSF													

Fig.31: Alignment of Human and R.affinis ACE2.

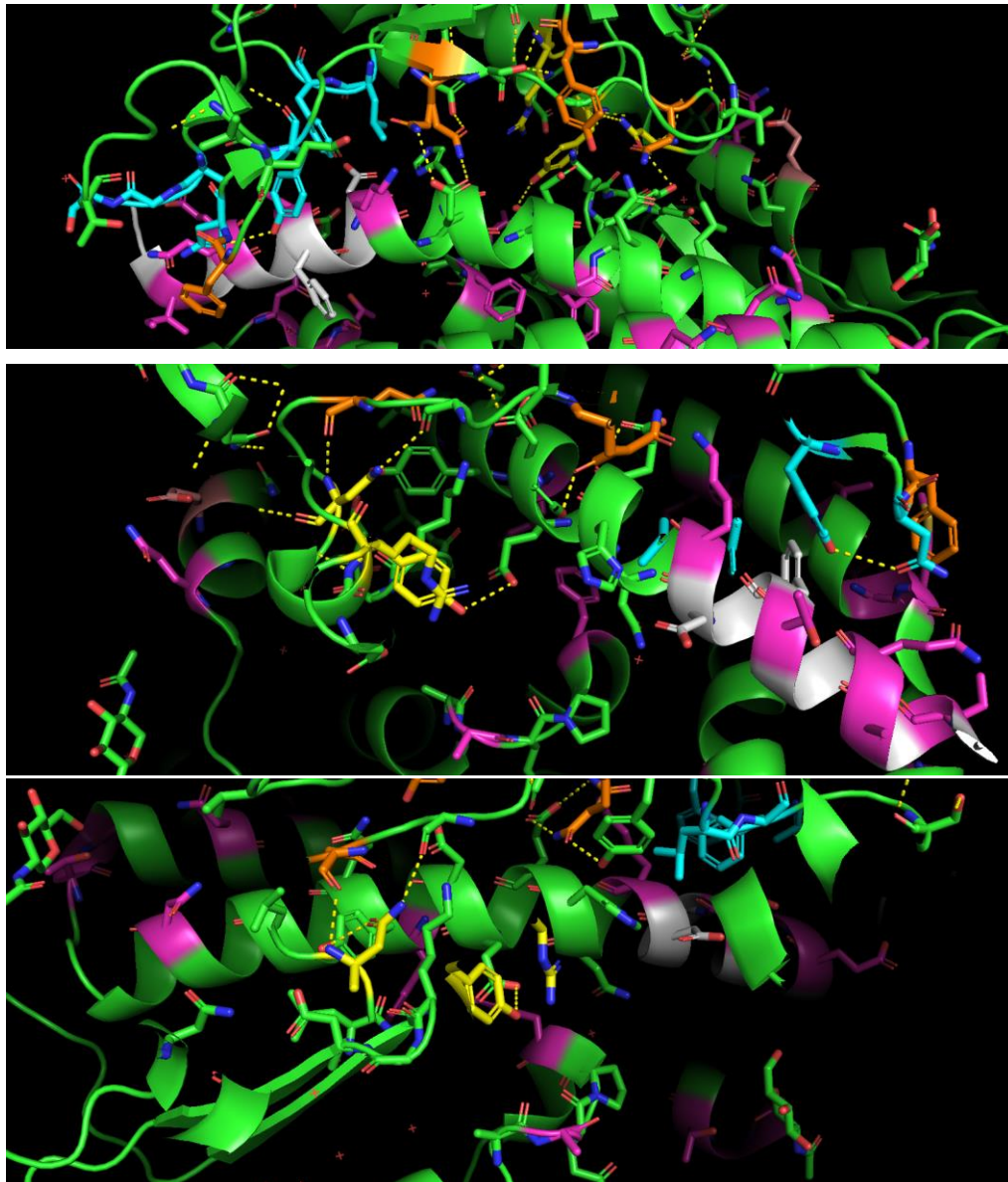


Fig.32: Structure of the pocket surrounding R403, Y449, N501 and Y505 on the SARS-CoV-2 RBD protein. Yellow is the R403, N501 and Y505 on SARS-CoV-2 RBD, green and white sticks denote residues that are identical between Human and R.affinis ACE2, Orange sticks denote residues that were different between SARS-CoV-2 and RaTG13 RBD and Magenta sticks denote residues that were different between human and R.affinis ACE2.

Consistent with the discovery of two residues (T403 and D501) with unique chemical properties that have never been recorded in any Sarbecoviruses, This reduction of binding affinity was found to be general for all animal ACE2 tested, with the highest recorded pseudovirus entry (RLU) being $\sim 10^1$ times lower than the entry efficiency of SARS-CoV-2 S on hACE2.

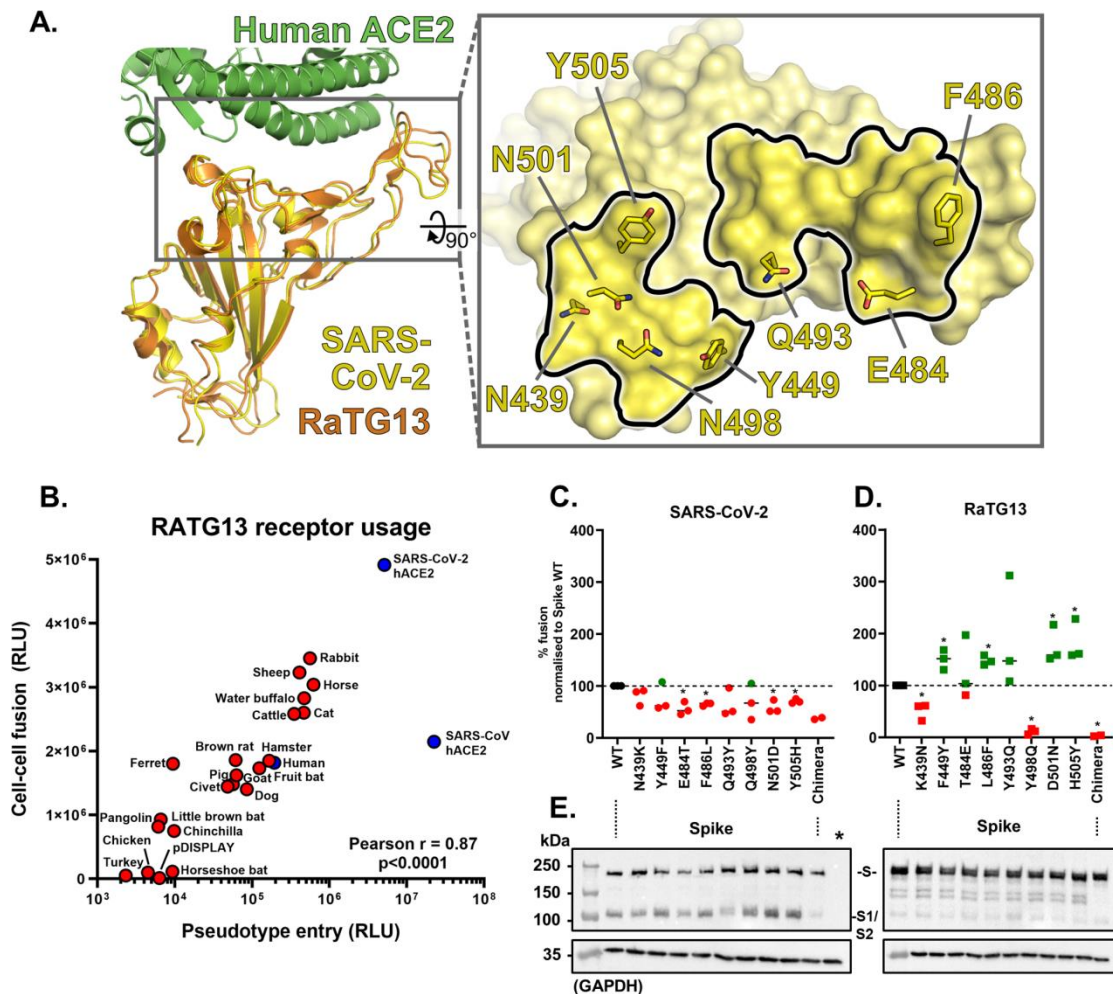


Fig.4 from [16]: Cell-to-cell fusion and pseudovirus entry assay of SARS-CoV-2, SARS-CoV and RaTG13 on different ACE2 orthologues overexpressed on HEK293T cells.

The RaTG13 S exhibits a restricted tropism and is specific to Immortalized Kidney cells.

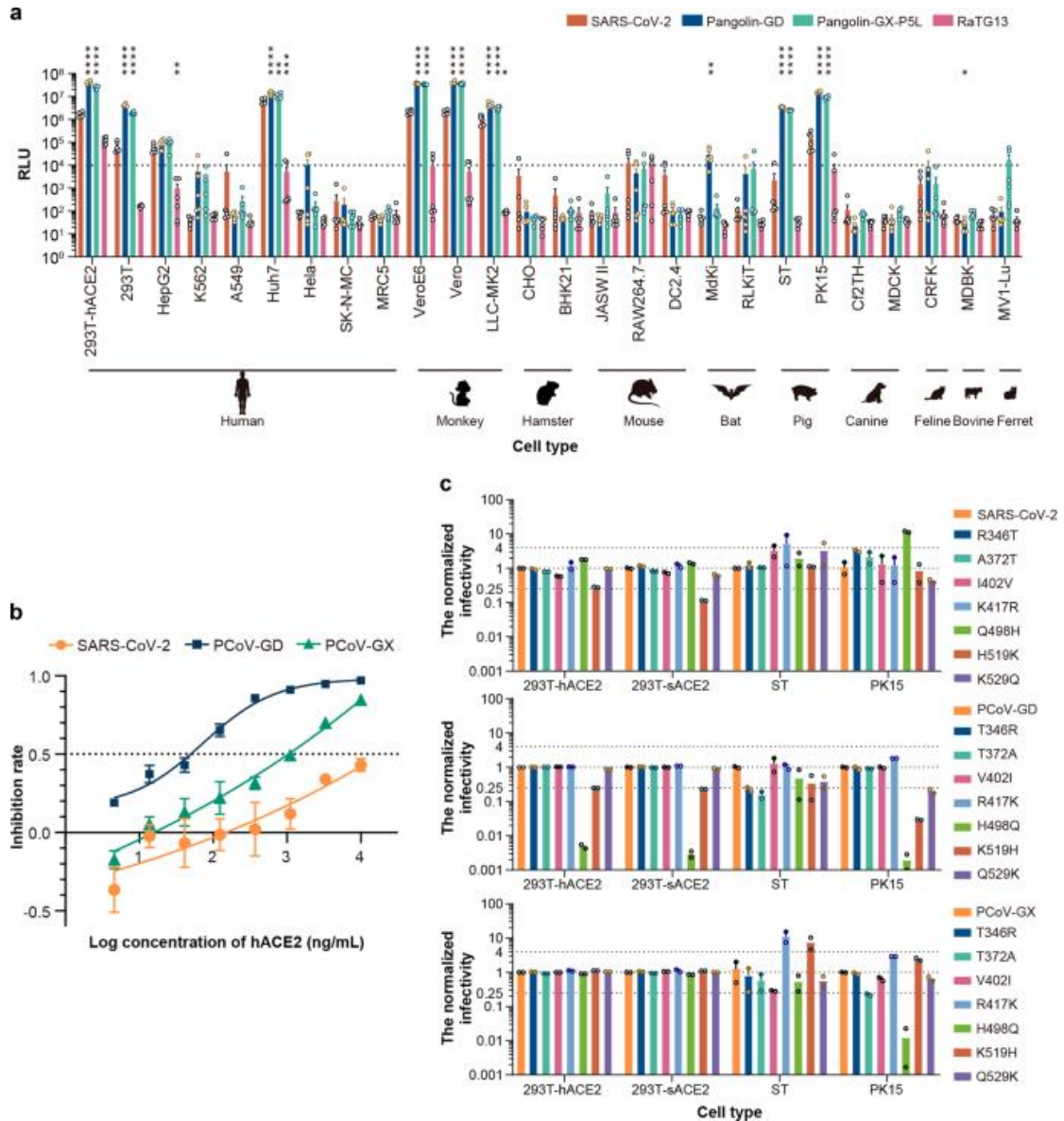


Fig.1 from [15] comparing the tropism of SARS-CoV-2, pCoV-GD, pCoV-GX and RaTG13. While only HEK293T-ACE2 displayed an infectivity for RaTG13 pseudovirus with an RLU of over 10⁴, both HEK293T-ACE2 and PK15 displayed a roughly 10¹ difference between the infectivity for SARS-CoV-2 and RaTG13. All other cell line where there RaTG13 show above-background infectivity, except for mouse Macrophage cell line RAW264.7, had a difference of 10² to 10³ in term of pseudovirus entry for SARS-CoV-2 and RaTG13, all with infectivity of SARS-CoV-2 significantly above that of RaTG13.

As ACE2 bind integrins through the KGD motif on position 353-355 which is conserved in human and *R.affinis* ACE2[17][18][19], It is modeled that ACE2 in physiological concentrations is bound to Integrin $\alpha 5 \beta 1$ and is inaccessible to binding by the RBD of Sarbecovirus Spike proteins[18],

unless it is displaced by an KGD/RGD motif that is found in all RBD sequences that lacked the two deletions in SL-CoVs RBDs that does not use ACE2 for entry.[20]

The primary feature of the HEK293T cells (ACE2) used in [11] is their substantially higher expression of ACE2 over their constitutional ITGB1 expression, which will result in large amount of free ACE2 that is physiologically unrealistic in real tissues like bat intestines or human lungs.

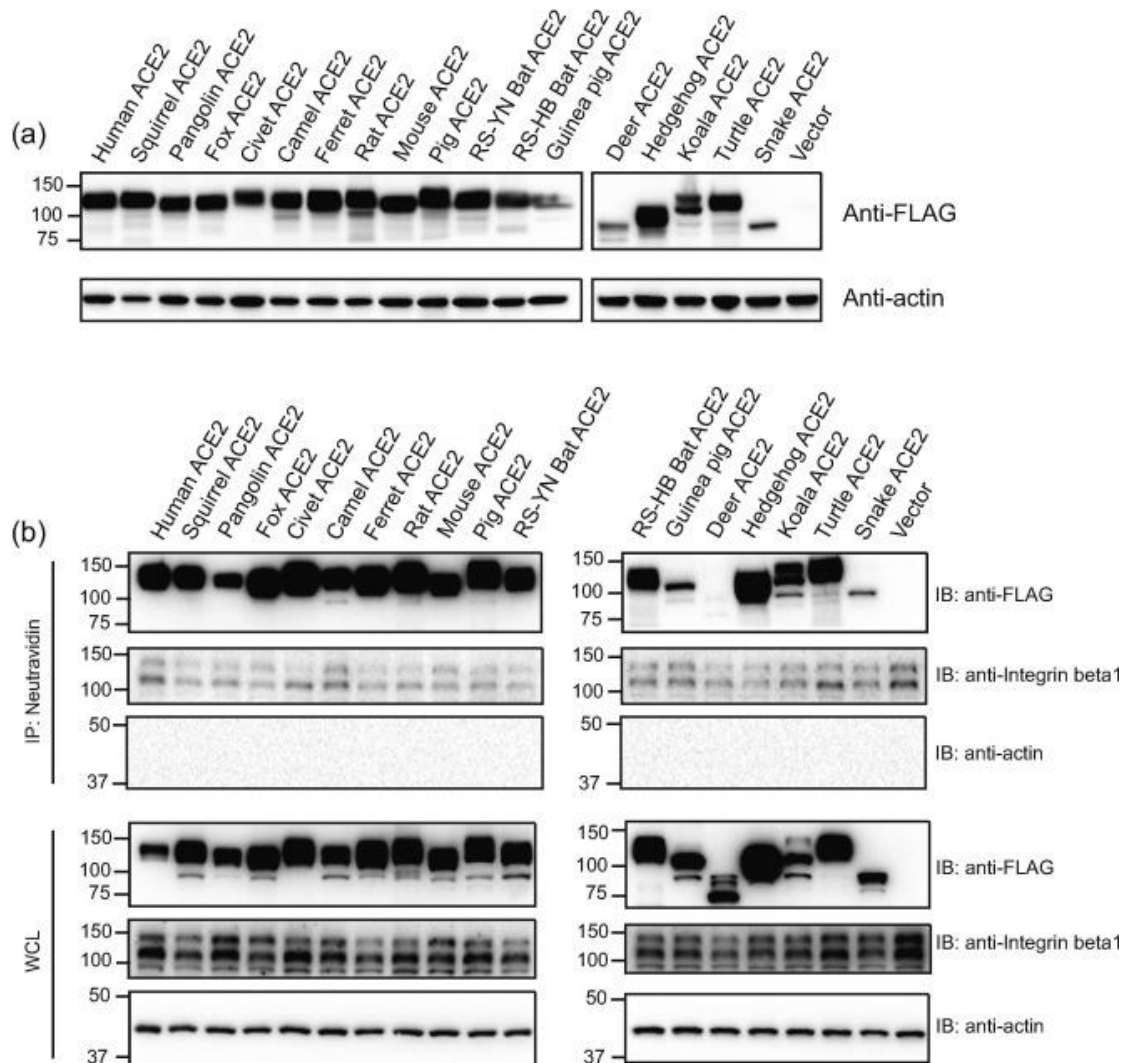


Fig.2 from [11]: Overexpression of ACE2 orthologues on HEK293T result in an overwhelmingly high amount of both whole-cell and surface ACE2 molecules comparing to the amount of ITGB1 molecules available for binding to ACE2.

Indeed, Inhibiting the interaction of the Spike to $\alpha 5 \beta 1$ integrins using an integrin-inhibiting peptide have been found to reduce the binding and entry efficiency of SARS-CoV-2 to hACE2 and VERO E6 cells[18], and Integrins have been speculated as a co-receptor for SARS-CoV-2[19][21].

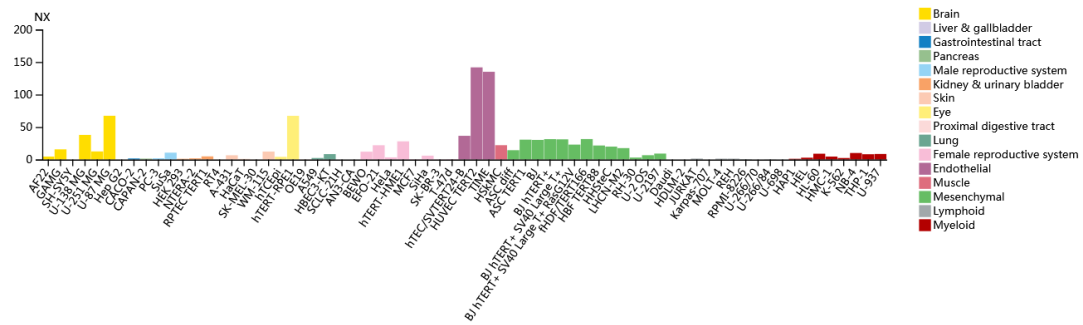


Fig.33a: expression level of ITGA5 on different cell lines.

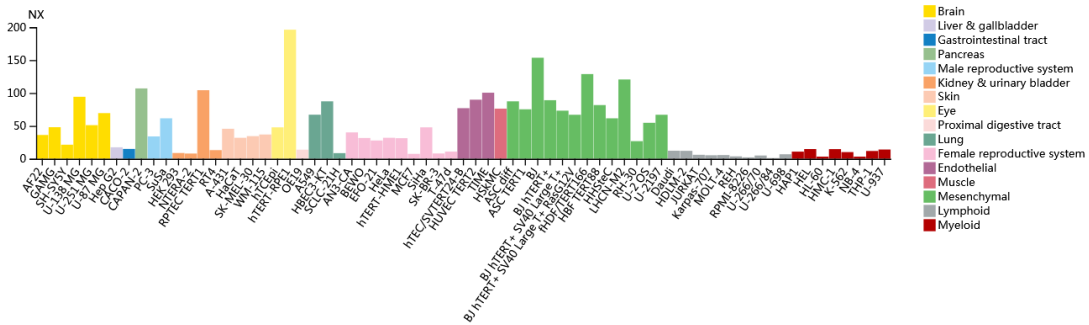


Fig.33b: expression level of ITGB1 on different cell lines.

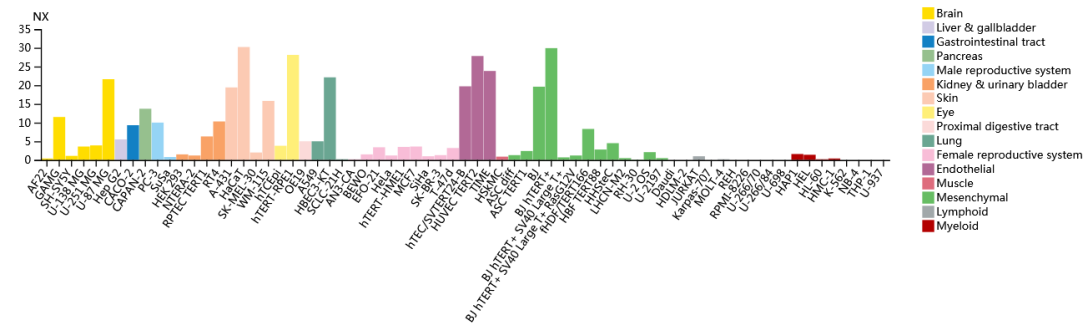


Fig.33c: expression level of ITGA3 on different cell lines.

The effect of integrin expression on the entry efficiency of RaTg13 and SARS-CoV-2 S pseudotyped lentivirus is demonstrated by the difference between the entry efficiency of the 3 Spike proteins to HeLa-ACE2 and HEK293T cells[22].

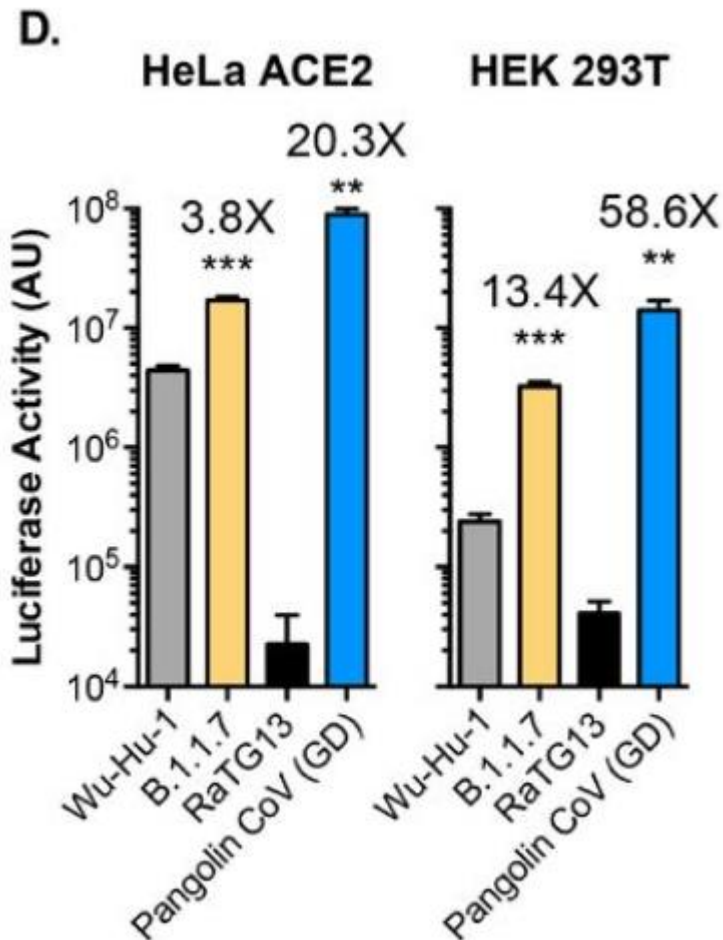


Fig.3d from[22]: HeLa ACE2 show substantially higher ratios between WuHu-1 or B1.1.7 entry and RaTG13 entry, compared to HEK293T.

As immortalized Kidney cells (HEK293T) are found to have much lower level of ITGB1, ITGA2 or ITGA5 expression, compounded with the fact that HEK293T-ACE2 cells is the only human cell line that support substantial entry by RaTG13 pseudotyped lentivirus with RLU above 10⁴[15] despite all cell lines from humans expressing only human ACE2, This highly restricted tropism of RaTg13 toward Immortalized Kidney cells likely indicate serial passage within such cells.

Incidentally, the only cell line from R.affinis in possession of the Wuhan Institute Of Virology (WIV) was RaK4324 cells from the Kidneys, which would have been the laboratory passage host for RaTG13 if it have been cultured prior to sequencing.[23]

As both the neutral 501 and the basic (R/K)403 are found to be 100% conserved in all Sarbecovirus RBD proteins except for RaTG13, these 2 positions are likely indispensable for the in-vivo fitness of Sarbecoviruses in both reservoir hosts, in other animals and in humans.

Since experimental evidence have validated the broadly detrimental effect of both D501 and T403 on the RaTG13 S on viral fitness (RBD binding to ACE2, Spike entry into cells), these two positions can be considered as signature of attenuation in the RaTG13 RBD protein.

RaTG13 is an attenuated vaccine strain cultured in immortalized bat kidney cells?

The only known cell line from *R.affinis* in possession of the Wuhan Institute of Virology was RaK4324 Primary Kidney cells[23], which were used in the isolation and culture of bat Coronaviruses.

Should the SRA dataset of RaTG13, SRX7724752, have been a cell culture of an attenuated virus within an immortalized version of the RaK4324 cells, It would simultaneously explain nearly all the known anomalies associated with the raw read data and the nucleotide sequence of RaTG13, MN996532.

Bat telomeres are known to not shorten with age[24], which indicate that the mechanism of telomere erosion is likely absent in bat cells. Should a traditional telomerase based immortalization strategy being used on a culture of *R.affinis* Kidney cells, one of the likely outcome is that telomeric sequences will grow uncontrollably and accumulate to very high fractions after extensive passage of the cell line due to the TERT activity not being balanced by telomere erosion mechanisms that were found in other mammalian cells but not bat cells.

In addition, Cell cultures are normally kept under sterile conditions using a cocktail of antibiotics in combination with aseptic techniques to minimize microbial growth, which would have resulted in a sample that is mostly sterile with minimal to no bacterial sequences.

One of the defining feature of the SARS-CoV-2 S is the optimization of ACE2 binding and folding at 37°C, a feature that it shares with the RaTG13 S.[26][27] However, the body temperature of a Horseshoe bat can reach up to 41°C[28], where substantial unfolding of the RaTG13 Spike happens according to Differential Scanning Fluorimetry on the Spike trimer[27]. This is incompatible with the high body temperature of a horseshoe bat (as the virus will be inactivated by the heat generated by bat flight), but is compatible with a cell culture as most cells in laboratories are cultured at 37°C.

Traces of lentivirus- and HERV-like fragments found in SRX7724752 likely indicate the usage of retroviral- and lentiviral- vectors on the sample, which are frequently used for the delivery of a TERT gene for the immortalization of cell lines in-vitro, a pre-requisite for the subsequent culture and attenuation for a vaccine strain.

Indeed, the combined features of the RaTG13 genome resemble that of a Live Attenuated Vaccine (LAV) almost suspiciously, to the point that there are actual proposals for the usage of this sequence as a candidate vaccine against SARS-CoV-2[25].

In addition, evidence of mutagen usage during the divergent evolution of RaTG13 and SARS-CoV-2 from a common ancestor can be found in the Spike protein CDS of RaTG13, manifesting as a very large excess of C:T transitions compared to the substitutional pattern of SARS-CoV-2 WIV04:ZC45, RaTG13:ZC45 or SARS-CoV Tor2:WIV1 on the aligned sections of their Spike protein CDS sequences.[29] As Mutagens like 5-fluorouracil is not present in wild bats, The RaTG13 Spike protein CDS would have to be grown in a cell culture to be influenced by 5-fluorouracil and show such a peculiar substitutional pattern.

CONCLUSION

The raw data of BtCoV/RaTG13 Contained multiple anomalies that signifies that the original sample could not have contained enough RNA template for the extraction of a complete viral genome as in MN996532.1

Furthermore, many of these anomalies points toward the fraudulent use of a mixed DNA library, rather than genuine mRNA, for the sequencing of SRX7724752, evident by the presence of widespread A-T ligation of unrelated dsDNA fragments that can only happen if the same library preparation process have been ran on dsDNA instead of ssRNA. which would constitute Academic fraud.

The Spike glycoprotein of RaTG13 does not resemble that of a wild virus but instead possessed multiple signatures of artificial attenuation in a cell culture when compared to the SARS-CoV-2 Spike and the Spike sequences of other related viruses, indicating that the sequence did not derive from what the Wuhan Institute Of Virology claimed to be.

Therefore, the sequencing of BtCoV/RaTG13 cannot be considered to be valid or honest as is, and any publications, including [2], and other publications that cites or use RaTG13 as critical pieces of evidence or proof, must be immediately invalidated and retracted.

REFERENCES

- [1] <https://www.thetimes.co.uk/article/seven-year-covid-trail-revealed-l5vxt7jqp>
- [2] Zhou P, Yang XL, Wang XG, et al. A pneumonia outbreak associated with a new coronavirus of probable bat origin. *Nature*. 2020;579(7798):270-273. doi:10.1038/s41586-020-2012-7
- [3] Rose C, Parker A, Jefferson B, Cartmell E. The Characterization of Feces and Urine: A Review of the Literature to Inform Advanced Treatment Technology. *Crit Rev Environ Sci Technol*. 2015;45(17):1827-1879. doi:10.1080/10643389.2014.1000761
- [4] <https://telegra.ph/RaTG13-07-06>
- [5] Xiao C, Li X, Liu S, Sang Y, Gao SJ, Gao F. HIV-1 did not contribute to the 2019-nCoV genome. *Emerg Microbes Infect*. 2020;9(1):378-381. Published 2020 Feb 14. doi:10.1080/22221751.2020.1727299
- [6] <https://www.planetnatural.com/product/mexican-bat-guano/>
- [7] Paskey, A.C., Frey, K.G., Schroth, G. *et al*. Enrichment post-library preparation enhances the sensitivity of high-throughput sequencing-based detection and characterization of viruses from complex samples. *BMC Genomics* **20**, 155 (2019). <https://doi.org/10.1186/s12864-019-5543-2>
- [8] Edgar, R. C. *et al*. Petabase-scale sequence alignment catalyses viral discovery. *bioRxiv* 2020.08.07.241729 (2020) [doi:10.1101/2020.08.07.241729](https://doi.org/10.1101/2020.08.07.241729)
- [9] Study of the Metatranscriptome of Eight Social and Solitary Wild Bee Species Reveals Novel Viruses and Bee Parasites
Karel Schoonvaere^{1,2*}, Guy Smaghe³, Frédéric Francis² and Dirk C. de Graaf¹

¹Laboratory of Molecular Entomology and Bee Pathology, Department of Biochemistry and Microbiology, Faculty of Sciences, Ghent University, Ghent, Belgium

²Functional and Evolutionary Entomology, Gembloux Agro-Bio Tech, University of Liege, Gembloux, Belgium

³Laboratory of Agrozoology, Department of Crop Protection, Faculty of Bioscience Engineering, Ghent University, Ghent, Belgium

[10] Zhang, S., Qiao, S., Yu, J. *et al.* Bat and pangolin coronavirus spike glycoprotein structures provide insights into SARS-CoV-2 evolution. *Nat Commun* **12**, 1607 (2021). <https://doi.org/10.1038/s41467-021-21767-3>

[11] Pei Li, Ruixuan Guo, Yan Liu, Yingtao Zhang, Jiixin Hu, Xiuyuan Ou, Dan Mi, Ting Chen, Zhixia Mu, Yelin Han, Zihan Chen, Zhewei Cui, Leiliang Zhang, Xinquan Wang, Zhiqiang Wu, Jianwei Wang, Qi Jin, Zhaohui Qian,

The *Rhinolophus affinis* bat ACE2 and multiple animal orthologs are functional receptors for bat coronavirus RaTG13 and SARS-CoV-2,

Science Bulletin,

2021,

,

ISSN 2095-9273,

<https://doi.org/10.1016/j.scib.2021.01.011>.

[12] Andersen, K.G., Rambaut, A., Lipkin, W.I. *et al.* The proximal origin of SARS-CoV-2. *Nat Med* **26**, 450–452 (2020). <https://doi.org/10.1038/s41591-020-0820-9>

[13] Makowski, L.; Olson-Sidford, W.; W. Weisel, J. Biological and Clinical Consequences of Integrin Binding via a Rogue RGD Motif in the SARS CoV-2 Spike Protein. *Viruses* **2021**, *13*, 146. <https://doi.org/10.3390/v13020146>

[14] Tyler N. Starr, Allison J. Greaney, Sarah K. Hilton, Daniel Ellis, Katharine H.D. Crawford, Adam S. Dingens, Mary Jane Navarro, John E. Bowen, M. Alejandra Tortorici, Alexandra C. Walls, Neil P. King, David Veessler, Jesse D. Bloom,

Deep Mutational Scanning of SARS-CoV-2 Receptor Binding Domain Reveals Constraints on Folding and ACE2 Binding,

Cell,

Volume 182, Issue 5,

2020,

Pages 1295-1310.e20,

ISSN 0092-8674,

<https://doi.org/10.1016/j.cell.2020.08.012>.

[15] Nie, J., Li, Q., Zhang, L. *et al.* Functional comparison of SARS-CoV-2 with closely related pangolin and bat coronaviruses. *Cell Discov* **7**, 21 (2021). <https://doi.org/10.1038/s41421-021-00256-3>

[16] Conceicao C, Thakur N, Human S, Kelly JT, Logan L, Bialy D, Bhat S, Stevenson-Leggett P, Zagrajek AK, Hollinghurst P, Varga M, Tsigoti C, Tully M, Chiu C, Moffat K, Silesian AP, Hammond JA, Maier HJ, Bickerton E, Shelton H, Dietrich I, Graham SC, Bailey D. The SARS-CoV-2 Spike protein has a broad tropism for mammalian ACE2 proteins. *PLoS Biol.* 2020 Dec 21;18(12):e3001016. doi: 10.1371/journal.pbio.3001016. PMID: 33347434; PMCID: PMC7751883.

[17] Clarke NE, Fisher MJ, Porter KE, Lambert DW, Turner AJ. Angiotensin converting enzyme (ACE) and ACE2 bind integrins and ACE2 regulates integrin signalling. *PLoS One.* 2012;7(4):e34747. doi: 10.1371/journal.pone.0034747. Epub 2012 Apr 16. PMID: 22523556; PMCID: PMC3327712.

[18] Brandon J. Beddingfield, Naoki Iwanaga, Prem P. Chapagain, Wenshu Zheng, Chad J. Roy, Tony Y. Hu, Jay K. Kolls, Gregory J. Bix,

The Integrin Binding Peptide, ATN-161, as a Novel Therapy for SARS-CoV-2 Infection,

JACC: Basic to Translational Science,
Volume 6, Issue 1,
2021,
Pages 1-8,
ISSN 2452-302X,
<https://doi.org/10.1016/j.jacbts.2020.10.003>.

[19] Factors Associated with Emerging and Re-emerging of SARS-CoV-2 Variants

Austin N. Spratt, Saathvik R. Kannan, Lucas T. Woods, Gary A. Weisman, Thomas P. Quinn, Christian L. Lorson, Anders Sönnnerborg, Siddappa N. Byrareddy, Kamal Singh
bioRxiv 2021.03.24.436850; doi: <https://doi.org/10.1101/2021.03.24.436850>

[20]

Difference in Receptor Usage between Severe Acute Respiratory Syndrome (SARS) Coronavirus and SARS-Like Coronavirus of Bat Origin

Wuze Ren, Xiuxia Qu, Wendong Li, Zhenggang Han, Meng Yu, Peng Zhou, Shu-Yi Zhang, Lin-Fa Wang, Hongkui Deng, Zhengli Shi

Journal of Virology Jan 2008, 82 (4) 1899-1907; DOI: 10.1128/JVI.01085-07

[21] Tikam Chand Dakal,

SARS-CoV-2 attachment to host cells is possibly mediated via RGD-integrin interaction in a calcium-dependent manner and suggests pulmonary EDTA chelation therapy as a novel treatment for COVID 19,

Immunobiology,
Volume 226, Issue 1,
2021,
152021,
ISSN 0171-2985,
<https://doi.org/10.1016/j.imbio.2020.152021>.

[22] Characterisation of B.1.1.7 and Pangolin coronavirus spike provides insights on the evolutionary trajectory of SARS-CoV-2

Samuel J. Dicken, Matthew J. Murray, Lucy G. Thorne, Ann-Kathrin Reuschl, Calum Forrest, Maaroothen Ganeshalingham, Luke Muir, Mphatso D. Kalempera, Machaela Palor, Laura E. McCoy, Clare Jolly, Greg J. Towers, Matthew B. Reeves, Joe Grove

bioRxiv 2021.03.22.436468; doi: <https://doi.org/10.1101/2021.03.22.436468>

[23] Wang N, Luo C, Liu H, Yang X, Hu B, Zhang W, Li B, Zhu Y, Zhu G, Shen X, Peng C, Shi Z. Characterization of a New Member of Alphacoronavirus with Unique Genomic Features in Rhinolophus Bats. *Viruses*. 2019 Apr 24;11(4):379. doi: 10.3390/v11040379. PMID: 31022925; PMCID: PMC6521148.

[24] Growing old, yet staying young: The role of telomeres in bats' exceptional longevity

By Nicole M. Foley, Graham M. Hughes, Zixia Huang, Michael Clarke, David Jebb, Conor V. Whelan, Eric J. Petit, Frédéric Touzalin, Olivier Farcy, Gareth Jones, Roger D. Ransome, Joanna Kacprzyk, Mary J. O'Connell, Gerald Kerth, Hugo Rebelo, Luísa Rodrigues, Sébastien J. Puechmaille, Emma C. Teeling

Science Advances 07 Feb 2018 : eaao0926

[25] Chougle, Afreen and Chougle, Humera and Sayyed, Rajat, Prospect of Using RaTG13 Sarbecovirus As a Candidate Vaccine for COVID-19 (September 2, 2020). Available at SSRN: <https://ssrn.com/abstract=3685067> or <http://dx.doi.org/10.2139/ssrn.3685067>

[26] Zhonghua Zhou, Ziyi Yang, Junxian Ou, Hong Zhang, Qiwei Zhang, Ming Dong, Gong Zhang, Temperature dependence of the SARS-CoV-2 affinity to human ACE2 determines COVID-19 progression and clinical outcome,

Computational and Structural Biotechnology Journal,

Volume 19,

2021,

Pages 161-167,

ISSN 2001-0370,

<https://doi.org/10.1016/j.csbj.2020.12.005>.

[27] Wrobel, A.G., Benton, D.J., Xu, P. *et al.* SARS-CoV-2 and bat RaTG13 spike glycoprotein structures inform on virus evolution and furin-cleavage effects. *Nat Struct Mol Biol* **27**, 763–767 (2020). <https://doi.org/10.1038/s41594-020-0468-7>

[28] O'Shea TJ, Cryan PM, Cunningham AA, Fooks AR, Hayman DT, Luis AD, Peel AJ, Plowright RK, Wood JL. Bat flight and zoonotic viruses. *Emerg Infect Dis.* 2014 May;20(5):741-5. doi: 10.3201/eid2005.130539. PMID: 24750692; PMCID: PMC4012789.

[29] Lv Longxian, Li Gaolei, Chen Jinhui, Liang Xinle, Li Yudong Comparative Genomic Analyses Reveal a Specific Mutation Pattern Between Human Coronavirus SARS-CoV-2 and Bat-CoV RaTG13 *Frontiers in Microbiology* vol.11 2020

<https://www.frontiersin.org/article/10.3389/fmicb.2020.584717>

<https://doi.org/10.3389/fmicb.2020.584717>

ISSN: 1664-302X